Audio Engineering Society

Convention Paper

Presented at the 129th Convention

2010 November 4–7 San Francisco, CA, USA

A Performance Ranking of Seven Different Types of Loudspeaker Line Arrays

D. B. (Don) Keele, Jr.[1]

[1] DBK Associates and Labs, Bloomington, Indiana 47408, USA
DKeeleJr@Comcast.net

ABSTRACT

Seven types of loudspeaker line arrays were ranked considering eight performance parameters including 1) Beamwidth uniformity, 2) Directivity uniformity, 3) Sound field uniformity, 4) Side lobe suppression, 5) Uniformity of polar response, 6) Smoothness of off-axis frequency response, 7) Sound pressure rolloff versus distance, and 8) Near-far polar pattern uniformity. Line arrays analyzed include: 1. Un-shaded straight-line array, 2. Hann-shaded straight-line array, 3. "J"-line array, 4. Spiral- or progressive-line array, 5. Un-shaded circular-arc array, 6. CBT circular-arc array, and 7.CBT delay-curved straight-line array. All arrays were analyzed assuming no extra drive signal processing other than frequency-independent shading. A weighted performance analysis yielded the following ranking from best to worse 6, 7, 5, 4, 3, 2, 1, with the CBT Legendre-shaded circular-arc array on top and the un-shaded straight-line array on the bottom.

1. INTRODUCTION

This paper analyzes and compares the performance of seven different types of loudspeaker line arrays using point-source "Huygens" computer modeling [1]. The arrays were then ranked with respect to each other according to their simulated performance.

1.1. Arrays Analyzed

Figure 1 shows the seven types of arrays that were analyzed and ranked. These arrays are listed in the following:

1. An un-shaded straight-line array [3, 4],
2. A Hann-shaded straight-line array [5],
3. An un-shaded "J"-line array with straight top half and circular-arc bottom half [6],
4. An un-shaded spiral- or progressive-line array [6],
5. An un-shaded circular-arc array [2, 7],
6. A Legendre-shaded CBT circular-arc array [2, 8-12], and beamwidth (bottom).and
7. A Legendre-shaded delay-curved CBT straight-line array [9].

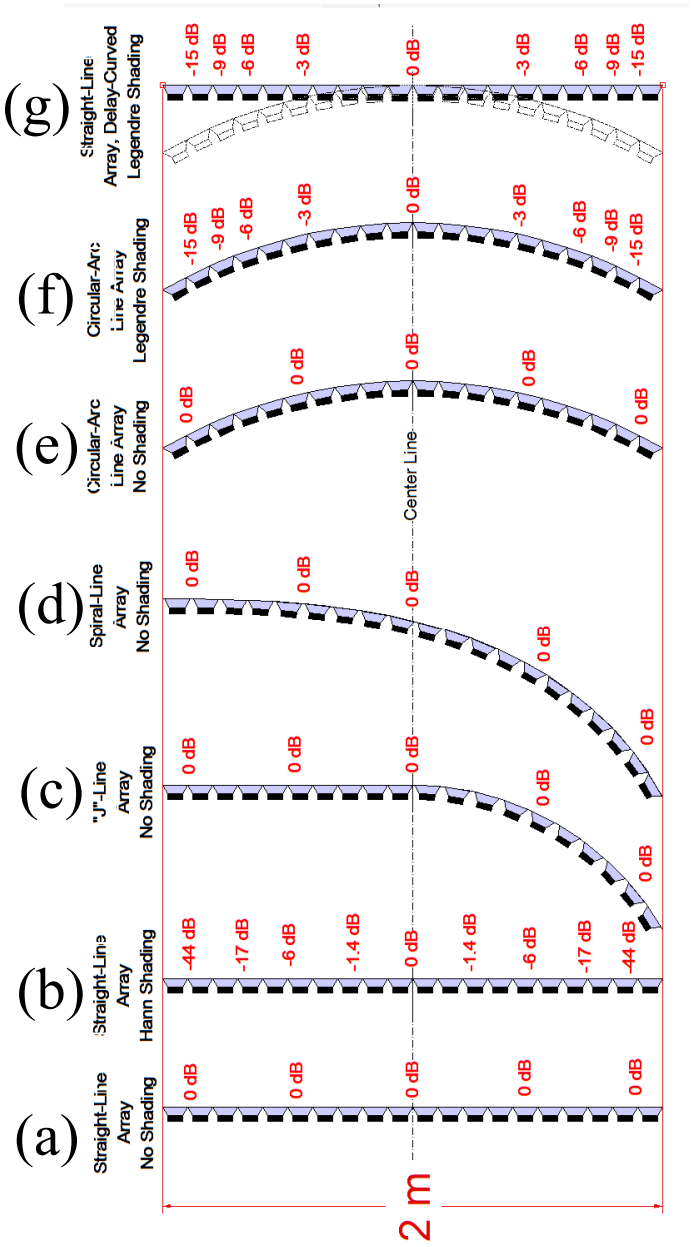

Fig. 1. Side views of seven types of loudspeaker line arrays that were compared via simulation. All arrays are 2 m high and are composed of 100 point sources. Source center-to-center spacing is about 20 mm (0.8 in). (Only 20 sources shown are shown on each array in this figure.) Approximate shading values in dB are shown on each array. From left to right, the arrays compared are: a) An un-shaded straight-line array. b) A Hann-shaded straight-line array. c) An un-shaded "J"-line array with straight top half and circular-arc bottom half. d) An un-shaded spiral- or progressive-line array. e) An un-shaded circular-arc array. f) A Legendre-shaded CBT circular-arc array, and g) A Legendre-shaded delay-curved CBT straight-line array with phantom delayed array shown in grey.

1.2. Array Simulation Conditions

All modeled arrays were 2m high and composed of 100 equal-spaced point sources. Source-to-source spacing was about 20 mm. This number of sources means that the simulated array can be considered as essentially continuous to about 12.5 kHz. Above this frequency, grating lobes appear due to the finite spacing of the sources being significant with respect to wavelength [13].

Each of the circular-arc arrays were 60°. The delay-curved CBT straight-line array was also curved to 60°. The "J" array had a 1m tall straight top and a 1m tall 60° circular-arc bottom section. The last source of the spiral array had an angle of 60°.

No complicated signal processing was permitted except for frequency-independent inter-element shading and in-line equalization to flatten the frequency response at a specific location.

All data was calculated at one-third-octave intervals over the range of 20 Hz to 20 kHz, although not all calculated data is shown.

1.3. Performance Parameters Evaluated

Eight performance parameters were simulated for each array and subjectively ranked. These performance parameters included:

1) Beamwidth uniformity,
2) Directivity uniformity,
3) Vertical sound-field uniformity,
4) Polar side lobe suppression,
5) Uniformity of polar response,
6) Smoothness and flatness of off-axis frequency response,
7) Sound pressure rolloff versus distance, and
8) Near-far polar pattern uniformity.

These performance and evaluation parameters are briefly described in the following:

1) Beamwidth uniformity:
The -6 dB beamwidth of the array was evaluated to assess how constant it is with frequency in a prescribed bandwidth.

2) Directivity uniformity:
The directivity of the array was evaluated to assess how constant it is with frequency in a prescribed bandwidth.

3) Vertical sound-field uniformity:
The 2D sound field of the array in the vertical plane was evaluated in a 6m x 6m region in front of the array to assess how uniform it is with frequency.

4) Polar side lobe suppression:
The minimization of side lobes was evaluated over the operating frequency bandwidth of the array. Ideally an array should generate a main polar beam with no secondary side lobes.

5) Uniformity of polar response:
The polar response uniformity with frequency was evaluated in the main polar lobe of the array.

6) Smoothness and flatness of off-axis frequency response:
The array's off-axis frequency response was assessed by grading its flatness and peak-to-peak ripple at different distances.

7) Sound pressure rolloff versus distance:
The sound pressure rolloff versus distance was evaluated to assess the uniformity of the rolloff. Ideally, the rolloff should be approximately the same at all frequencies in the operating bandwidth of the array (except for a possible level change from frequency to frequency). This means that if the frequency response is equalized flat at a specific distance in front of the array, it will be equally flat at other distances, nearer and farther away.

8) Near-far polar pattern uniformity.
The polar pattern of the array was evaluated for its uniformity with distance from points close to the array in the near field out to mid-field and far-field distances.

1.4. Performance Ranking

The subjective score of these eight parameters, on a scale from 1 to 10 with 10 highest, was evaluated for each array type. This numerical assessment was then combined into a weighted final evaluation score which allowed the arrays to be performance ranked with respect to each other.

2. ANALYSIS

This section presents the graphical results of the array's performance for each of the performance parameters and assigns a subjective numerical score.

2.1. Beamwidth uniformity:

The -6 dB beamwidth vs. frequency of each array was evaluated to assess how constant it is with frequency in a prescribed bandwidth of about 200 Hz to 12.5 kHz. The beamwidth was evaluated at a distance of 250 m, which is essentially in the far field for a 2m tall array.

The following seven figures show the -6 dB beamwidth vs. frequency for each of the arrays. Brief descriptive comments follow each figure describing the data.

2.1.1. Un-shaded straight-line array

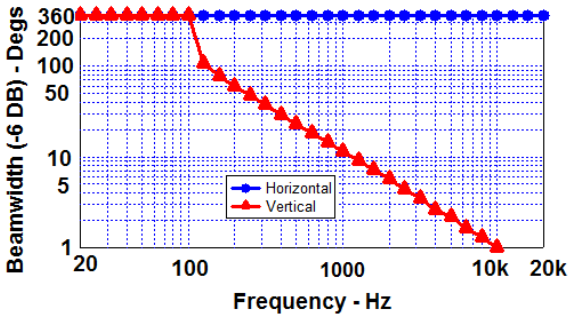

Fig. 2. Beamwidth of un-shaded straight-line array.

The vertical beamwidth of the un-shaded straight-line array continually falls with frequency above 125 Hz at a rate which halves with each doubling of frequency.

2.1.2. Hann-shaded straight-line array

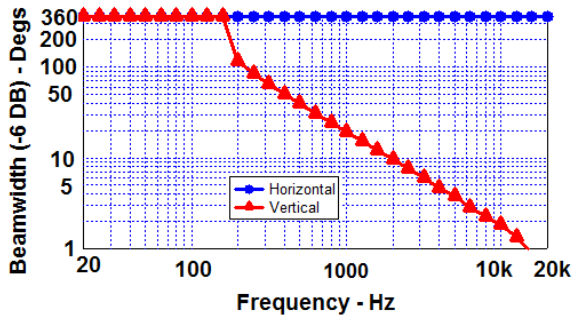

Fig. 3. Beamwidth of Hann-shaded straight-line array.

Like the previous un-shaded straight-line array, the beamwidth of the Hann-shaded array also falls with frequency, but starts at a higher frequency of 200 Hz. Effectively, the shading widens the beamwidth by about 60%.

2.1.3. Un-shaded "J"-line array with straight top half an circular-arc bottom half

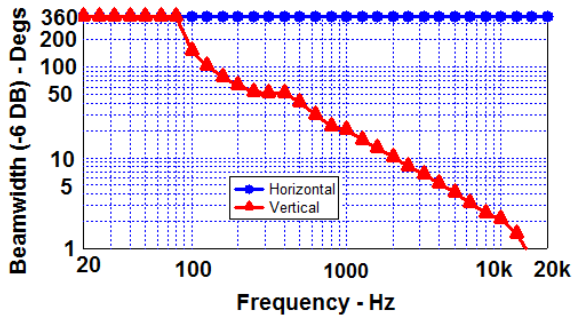

Fig. 4. Beamwidth of un-shaded "J"-line array.

Like the previous straight-line arrays, the beamwidth of the "J"-line array also falls with frequency, but with a slope that shifts gears at about 400 Hz. Below this frequency, the beamwidth follows the 60° curved-arc section , and above follows the straight-line section.

2.1.4. Un-shaded spiral-line array

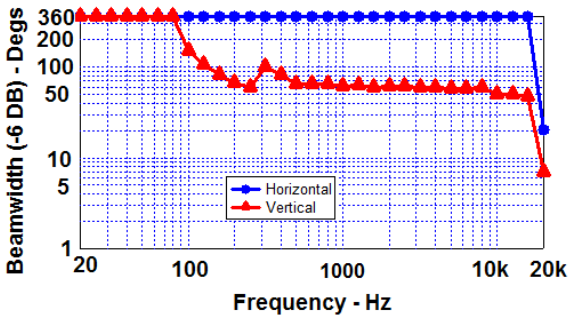

Fig. 5. Beamwidth of un-shaded spiral line array.

The beamwidth of the spiral-line array is quite constant at about 60° above 200 Hz except for a slight dip and peak at 250 and 315 Hz.

2.1.5. Un-shaded circular-arc line array

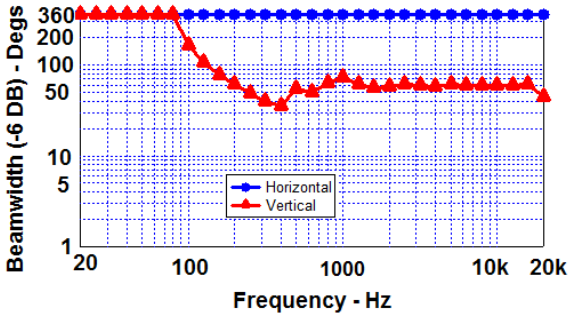

Fig. 6. Beamwidth of un-shaded circular-arc line array.

The beamwidth of the un-shaded circular-arc array is quite constant at about 60° above 500 Hz, but includes somewhat more deviations than the previous spiral-line array. The beamwidth reduction to about 35° at 400 Hz is the typical so called "midrange narrowing" that un-shaded circular-arc radiators exhibit.

2.1.6. Legendre-shaded CBT circular-arc line array

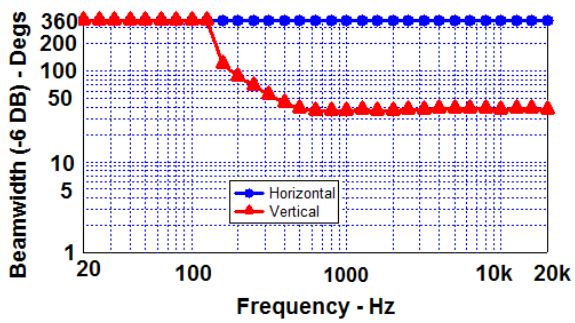

Fig. 7. Beamwidth of Legendre-shaded circular-arc (CBT) line array.

The beamwidth of the Legendre-shaded CBT circular-arc array is exceedingly uniform at about 40° above 400 Hz. Note that the shading has actually reduced the beamwidth as compared to the un-shaded circular-arc array. The beamwidth of an un-shaded circular-arc array is essentially equal to the arc angle (60° in this case). However, the beamwidth of a Legendre-shaded CBT circular-arc array is about 64% of the arc angle (40° in this case).

2.1.7. Legendre-shaded delay-curved CBT straight-line array

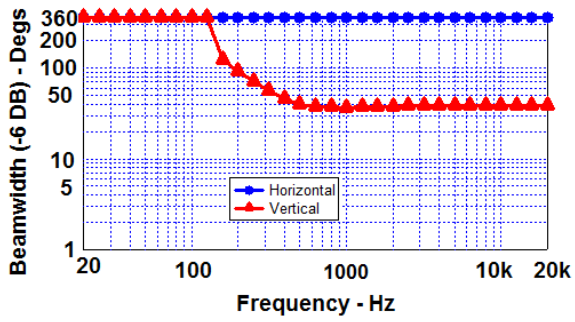

Fig. 8. Beamwidth of Legendre-shaded delay-curved CBT straight-line array.

In the far field, the beamwidth of the Legendre-shaded delay-curved CBT straight-line array is essentially equal to the beamwidth of the previous shaded circular-arc array and is equally uniform and well behaved.

2.1.8. Beamwidth uniformity ranking scores:

The following list shows the subjective scores I assigned to the beamwidth data for each of the arrays:

1. Un-shaded straight-line array: 2
2. Hann-shaded straight-line array: 2
3. Un-shaded "J"-line array: 1
4. Un-shaded spiral-line array: 9
5. Un-shaded circular-arc array: 8
6. Legendre-shaded CBT circular-arc array: 10
7. Legendre-shaded delay-curved CBT straight-line array: 10

2.1.9. Array ranking for beamwidth uniformity:

The following list rearranges the previous list of scores in rank order with highest rank on top and lowest on bottom.

1. Legendre-shaded CBT circular-arc array: 10
2. Legendre-shaded delay-curved CBT straight-line array: 10
3. Un-shaded spiral-line array: 9
4. Un-shaded circular-arc array: 8
5. Hann-shaded straight-line array: 2
6. Un-shaded straight-line array: 2
7. Un-shaded "J"-line array: 1

The circular-arc and delay-curved CBT arrays come out on top in this list with the spiral and un-shaded circular arc arrays a close second. The shaded and un-shaded straight-line arrays are on the bottom.

2.2. Directivity uniformity:

Each array's directivity index and Q vs. frequency was evaluated to assess how constant it is with frequency in a prescribed bandwidth of about 200 Hz to 12.5 kHz. The directivity was evaluated at a distance of 250m, which is essentially in the far field for a 2m tall array.

The following seven figures show the directivity of each of the arrays with brief comments following.

2.2.1. Un-shaded straight-line array

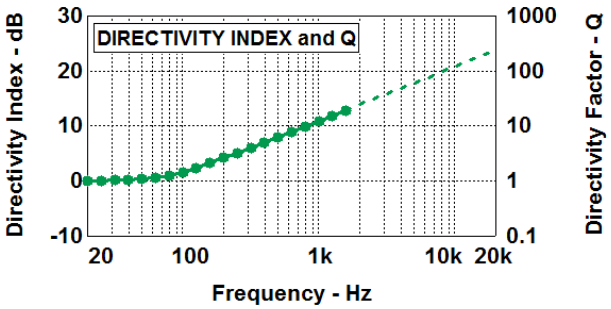

Fig. 9. Directivity of un-shaded straight-line array.

The directivity of both the un-shaded and shaded straight-line arrays (next figure) continually rises with frequency. The directivity rise at high frequencies was extrapolated (dashed line) because of the failure of the simulator in predicting the rise when the lobe widths drop below 1° (1°is the angular resolution of the simulator in calculating the directivity).

2.2.2. Hann-shaded straight-line array

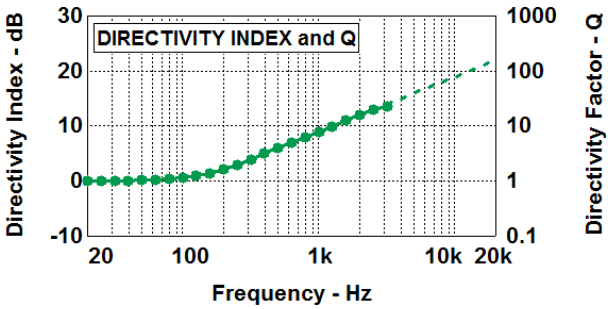

Fig. 10. Directivity of Hann-shaded straight-line array.

See comments after the previous figure. The Hann shading raises the point at which the directivity starts to rise by about 2/3rds octave.

2.2.3. Un-shaded "J"-line array

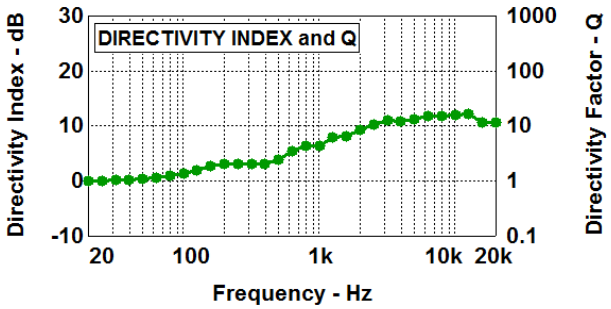

Fig. 11. Directivity of un-shaded "J"-line array.

The directivity of the "J"-line array reaches a roughly-constant plateau of about 10 dB above 2 kHz.

2.2.4. Un-shaded spiral-line array

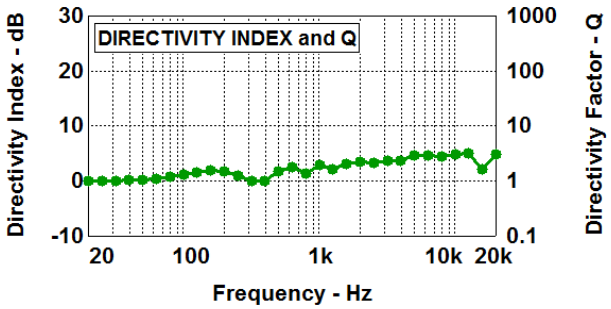

Fig. 12. Directivity of un-shaded spiral line array.

The directivity of the spiral-line array is relatively low over most of the range but continually rises above 500 Hz at a gradual rate.

2.2.5. Un-shaded circular-arc line array

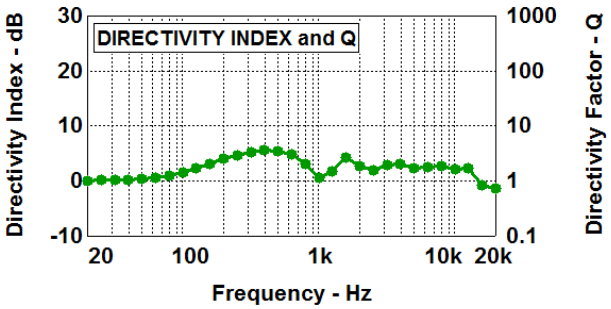

Fig. 13. Directivity of un-shaded circular-arc array.

The directivity of the un-shaded circular-arc array is also relatively low but exhibits much variation below 2 kHz.

2.2.6. Legendre-shaded CBT circular-arc line array

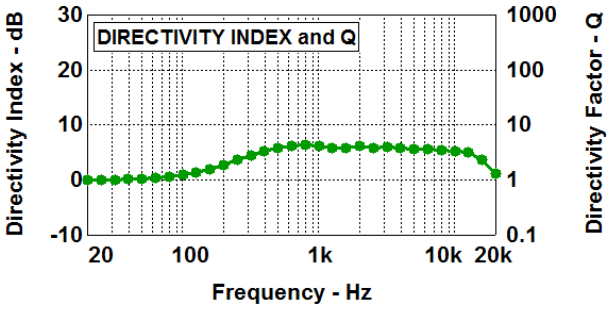

Fig. 14. Directivity of Legendre-shaded CBT circular-arc array.

The directivity of the shaded circular-arc array is moderately high at about 6-7 dB and is very constant and well behaved above 400 Hz.

2.2.7. Legendre-shaded delay-curved CBT straight-line array

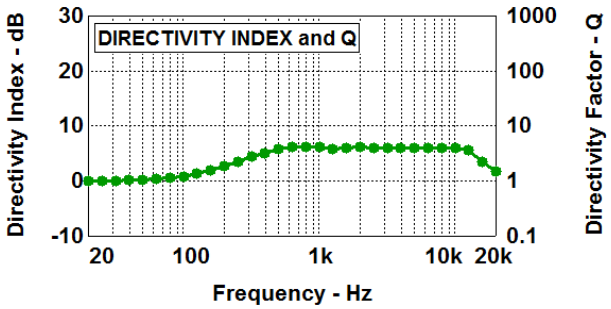

Fig. 15. Directivity of Legendre-shaded delay-curved CBT straight-line array.

The directivity of the shaded delay-curved straight-line array is also very well behaved and is essentially equal to the previous shaded CBT circular-arc array.

2.2.8. Directivity uniformity ranking scores:

The following list shows the subjective scores I assigned to the directivity data of each of the arrays:

1. Un-shaded straight-line array: 1
2. Hann-shaded straight-line array: 1
3. Un-shaded "J"-line array: 4
4. Un-shaded spiral- or progressive-line array: 7
5. Un-shaded circular-arc array: 5
6. Legendre-shaded CBT circular-arc array: 10
7. Legendre-shaded delay-curved CBT straight-line array: 10

2.2.9. Array ranking for directivity uniformity:

The following list ranks the arrays according to their directivity scores with the highest rank on top:

1. Legendre-shaded CBT circular-arc array: 10
2. Legendre-shaded delay-curved CBT straight-line array: 10
3. Un-shaded spiral- or progressive-line array: 7
4. Un-shaded circular-arc array: 5
5. Un-shaded "J"-line array: 4
6. Hann-shaded straight-line array: 1
7. Un-shaded straight-line array: 1

The circular-arc and delay-curved CBT arrays also come out on top when directivity is considered, with the spiral, "J"-line, and un-shaded circular arc arrays in the middle of the ranking. As with the previous beamwidth rankings, the shaded and un-shaded straight-line arrays are on the bottom.

2.3. Vertical sound-field uniformity:

The 2D vertical-plane sound field of each array was evaluated in a 6m x 6m region in front of the array at third-octaves intervals from 63 Hz to 16 kHz. For ease of comparison, this section shows two frequencies at 1 kHz and 8 kHz for each array. Section 6 Appendix 1 shows a more complete sampling of these sound-fields at eight octaves from 125 Hz to 16 kHz for each array.

The complete sets of sound-field images for each array were then subjectively scored for uniformity of coverage.

2.3.1. Sound-field level color scale

The following scale illustrates the false colors used to indicate the sound pressure levels in dB ranging from -40 to +10 dB. Note that each sound-field image clearly shows the location and shading of the array in the left side of each display (in yellow indicating the high source SPL).

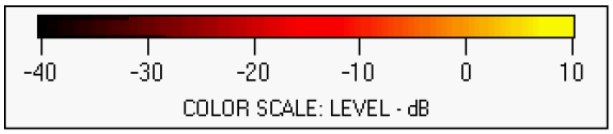

2.3.2. Un-shaded straight-line array

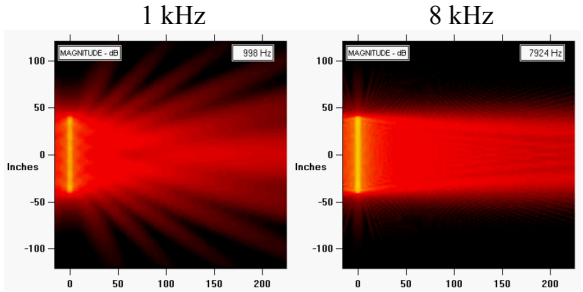

Fig. 16. Vertical sound-field displays for the un-shaded straight-line array at frequencies of 1 kHz (left) and 8 kHz (right).

The sound-field of the un-shaded straight-line array continually gets narrower and narrower with frequency and exhibits a considerable amount of side lobes at the lower frequencies.

2.3.3. Hann-shaded straight-line array

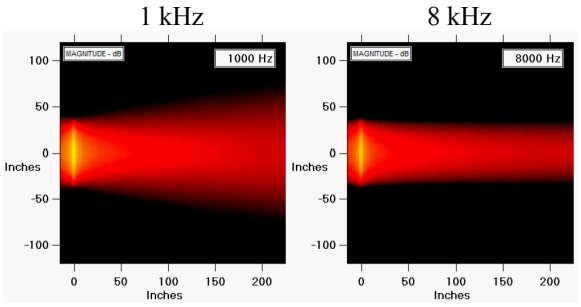

Fig. 17. Vertical sound-field displays for the Hann-shaded straight-line array at frequencies of 1 kHz (left) and 8 kHz (right).

Although the Hann-shaded straight-line array continually gets narrower and narrower with frequency, it does so with absolutely no side lobes.

2.3.4. Un-shaded "J"-line array with straight top half an circular-arc bottom half

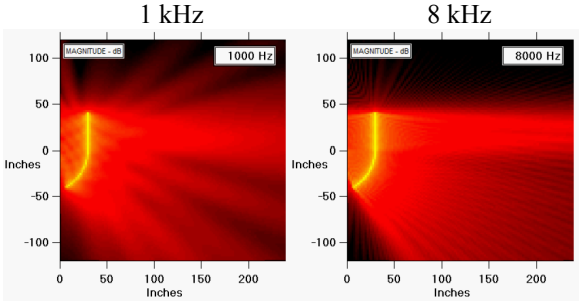

Fig. 18. Vertical sound-field displays for the un-shaded "J"-line array at frequencies of 1 kHz (left) and 8 kHz (right).

The sound-field of this array exhibits two distinct regions radiated by the two different sections that make up the array. The upper half radiates a pattern aimed straight to the right that continually gets narrower with frequency. The bottom circular-arc section radiates a roughly constant-beamwidth circular pattern equal to the 60° wedge angle. Both patterns exhibit a rich side-lobe structure that changes dramatically with frequency.

2.3.5. *Un-shaded spiral-line array*

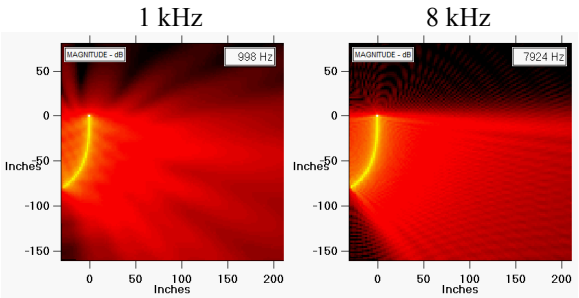

Fig. 19. Vertical sound-fields for the un-shaded spiral-line array at frequencies of 1 kHz (left) and 8 kHz (right).

The spiral-line array exhibits a somewhat constant beamwidth radiation pattern but that also exhibits a rich side-lobe structure that changes significantly with frequency.

2.3.6. *Un-shaded circular-arc line array*

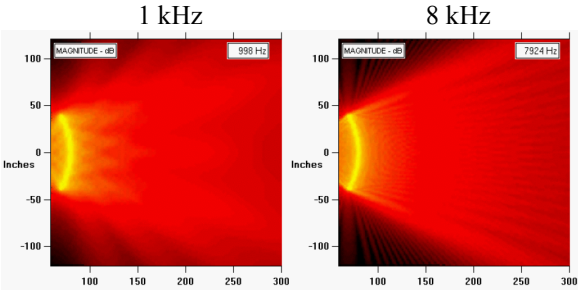

Fig. 20. Vertical sound-field displays for the un-shaded circular-arc line array at frequencies of 1 kHz (left) and 8 kHz (right).

The sound-field of the un-shaded circular-arc line array also exhibits a somewhat constant beamwidth with frequency but coupled with many side lobes. Note the rich detail in the pattern close to the array.

2.3.7. *Legendre-shaded CBT circular-arc line array*

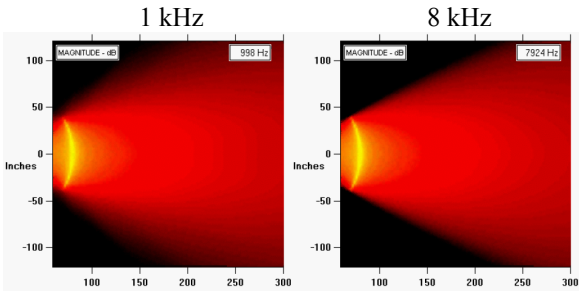

Fig. 21. Vertical sound-field displays for the Legendre-shaded CBT circular-arc line array at frequencies of 1 kHz (left) and 8 kHz (right).

The Legendre-shaded circular-arc line array exhibits a remarkably even sound-field with frequency with a beamwidth of about 64% of the circular-arc angle.

2.3.8. *Legendre-shaded delay-curved CBT straight-line array*

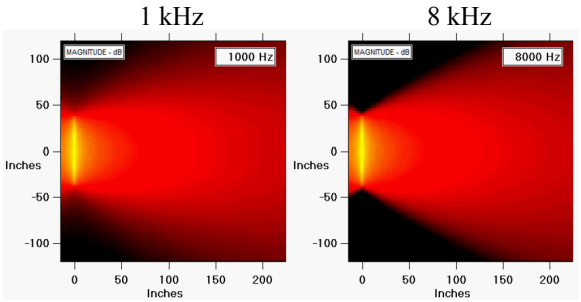

Fig. 22. Vertical sound-field displays for the Legendre-shaded delay-curved CBT straight-line array at frequencies of 1 kHz (left) and 8 kHz (right).

The Legendre-shaded delay-curved CBT straight-line array also exhibits a remarkably even sound-field with frequency the same as the previous Legendre-shaded circular-arc CBT line array

2.3.9. *Vertical sound-field uniformity ranking scores:*

The following shows the subjective scores I assigned to the sound-field information for each array:

1. Un-shaded straight-line array: 1
2. Hann-shaded straight-line array: 4
3. Un-shaded “J”-line array: 2
4. Un-shaded spiral- or progressive-line array: 2

5. Un-shaded circular-arc array: 4
6. Legendre-shaded CBT circular-arc array: 10
7. Legendre-shaded delay-curved CBT straight-line array: 10

2.3.10. Array ranking for vertical sound-field uniformity:

The following list ranks the arrays according to their sound-field uniformity scores with the highest ranked array on top:

1. Legendre-shaded CBT circular-arc array: 10
2. Legendre-shaded delay-curved CBT straight-line array: 10
3. Un-shaded circular-arc array: 4
4. Hann-shaded straight-line array: 4
5. Un-shaded spiral- or progressive-line array: 2
6. Un-shaded "J"-line array: 2
7. Un-shaded straight-line array: 1

As in the previous rankings, the circular-arc and delay-curved CBT arrays come out on top. The un-shaded circular arc array and the Hann-shaded straight-line arrays show up in the middle of the ranking. The un-shaded spiral and straight-line arrays ends up on the bottom.

2.4. Polar side lobe suppression:

The minimization of side lobes was evaluated over the operating frequency bandwidth of the array. Ideally an array should generate a main polar beam with no secondary side lobes.

Section 7 Appendix 2 shows a complete set of far-field (250 m) vertical polar curves at octave centers from 125 Hz to 16 kHz. These curves were selected from the complete set of third-octave polars simulated from 63 Hz to 16 kHz.

Each of these polars shows both sides of the polar, i.e. front and rear (right and left). The polar simulation uses point sources which radiate equally well to the rear. In the far-field, all these polars are right-left symmetric.

2.4.1. Polar side lobe suppression ranking scores:

The following shows the subjective scores I assigned to each array for side lobe suppression by examining the complete set of vertical third-octave polar curves:

1. Un-shaded straight-line array: 1
2. Hann-shaded straight-line array: 9
3. Un-shaded "J"-line array: 6
4. Un-shaded spiral- or progressive-line array: 7
5. Un-shaded circular-arc array: 7
6. Legendre-shaded CBT circular-arc array: 10
7. Legendre-shaded delay-curved CBT straight-line array: 10

2.4.2. Array ranking for polar side lobe suppression:

The following ranks the arrays according to their polar side lobe suppression scores with the highest ranked array on top:

1. Legendre-shaded CBT circular-arc array: 10
2. Legendre-shaded delay-curved CBT straight-line array: 10
3. Hann-shaded straight-line array: 9
4. Un-shaded circular-arc array: 7
5. Un-shaded spiral- or progressive-line array: 7
6. Un-shaded "J"-line array: 6
7. Un-shaded straight-line array: 1

Six of the seven arrays end up in the top half of the rankings with the CBT arrays on top and the un-shaded straight-line array on the bottom.

2.5. Uniformity of vertical polar response:

The polar response uniformity with frequency was evaluated examining the main lobe of the polar response from the complete set of third-octave polar curves. The same polars from the previous section in Section 8 Appendix 2 were examined to determine the polar response uniformity.

2.5.1. Vertical polar response uniformity ranking scores:

The following shows the subjective scores I assigned to each array for polar response uniformity by examining the complete set of third-octave polar curves:

1. Un-shaded straight-line array: 1
2. Hann-shaded straight-line array: 2
3. Un-shaded "J"-line array: 5
4. Un-shaded spiral- or progressive-line array: 6
5. Un-shaded circular-arc array: 6
6. Legendre-shaded CBT circular-arc array: 10
7. Legendre-shaded delay-curved CBT straight-line array: 10

2.5.2. Array ranking for polar response uniformity:

The following ranks the arrays according to their polar response uniformity scores with the highest ranked array on top:

1. Legendre-shaded CBT circular-arc array: 10
2. Legendre-shaded delay-curved CBT straight-line array: 10
3. Un-shaded circular-arc array: 6
4. Un-shaded spiral- or progressive-line array: 6
5. Un-shaded "J"-line array: 5
6. Hann-shaded straight-line array: 2
7. Un-shaded straight-line array: 1

When polar uniformity is considered, the CBT arrays end up on top with the Hann-shaded and un-shaded straight-line arrays on the bottom. The un-shaded circular-arc, the un-shaded spiral-line, and the un-shaded "J"-line arrays wind up in the middle.

2.6. Smoothness and flatness of off-axis frequency response:

Ideally, the off-axis frequency response should be well-behaved, smooth and flat, and be independent of distance. In order to assess this, the off-axis frequency response of the arrays was simulated at two distances of 3 m and 18 m. Frequency responses were simulated at six on- and off-axis angles from 0° to 30°, with a step of 6°, with the on-axis response equalized flat. The responses were color coded with the following colors:

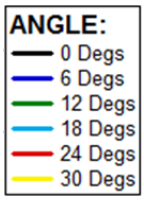

For most of the arrays, angular rotation was about the center of the array except for the circular-arc arrays where the rotation was about the center of curvature of the array.

The resultant array's off-axis frequency responses were then subjectively graded by judging the response flatness, uniformity, absence of ripple, etc.

2.6.1. Un-shaded straight-line array

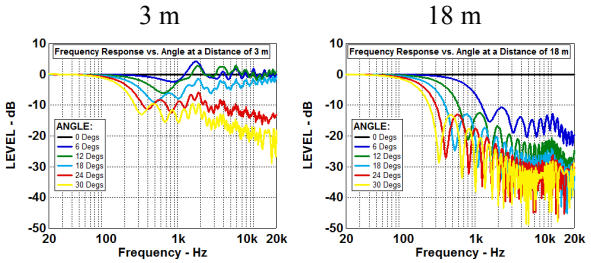

Fig. 23. Off-axis frequency responses of the un-shaded straight-line array at distances of 3 m (left) and 18 m (right).

The off-axis frequency response of the un-shaded straight-line array is very poor and exhibits considerable variation with frequency, angle, and distance. Ripple and peak-to-peak variation are very high in all responses.

2.6.2. Hann-shaded straight-line array

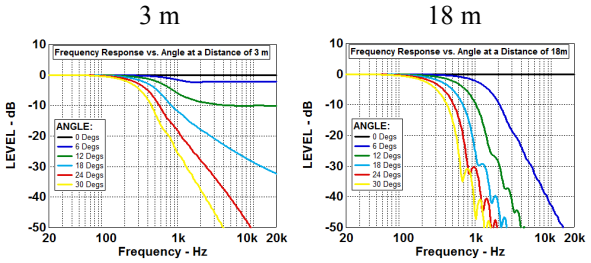

Fig. 24. Off-axis frequency responses of the Hann-shaded straight-line array at distances of 3 m (left) and 18 m (right).

Hann-shading essentially eliminates the ripple in the off-axis responses of the straight-line array. Unfortunately, the response curves themselves are still very non-uniform curve-to-curve and change very significantly with distance.

2.6.3. *Un-shaded "J"-line array with straight top half an circular-arc bottom half*

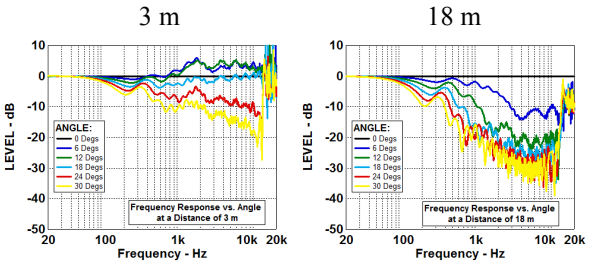

Fig. 25. Off-axis frequency responses of the un-shaded "J"-line array at distances of 3 m (left) and 18 m (right).

Similar to the un-shaded straight-line array, the off-axis frequency response of the un-shaded "J"-line array is very poor and exhibits considerable variation with frequency, angle, and distance.

2.6.4. *Un-shaded spiral-line array*

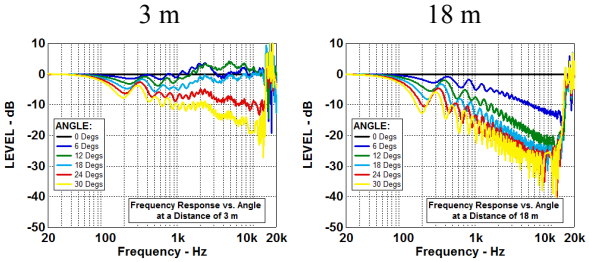

Fig. 26. Off-axis frequency responses of the un-shaded spiral-line array at distances of 3 m (left) and 18 m (right).

The off-axis responses of the spiral-line array are much improved as compared to the previous three arrays. Ripple is still quite significant, but the curve-to-curve variation is less. However, major response differences still exists at the two distances.

2.6.5. *Un-shaded circular-arc line array*

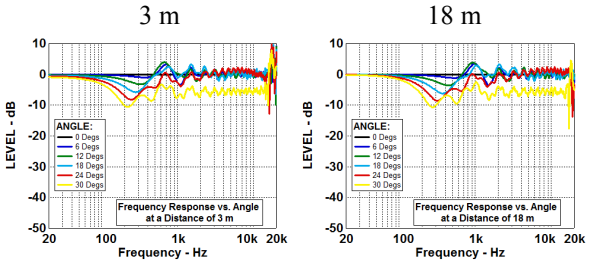

Fig. 27. Off-axis frequency responses of the un-shaded circular-arc line array at distances of 3 m (left) and 18 m (right).

Although much ripple and peak-to-peak variation exists in the off-axis responses of the un-shaded circular-arc line array, the response variation and flatness is much superior to the previous arrays. In addition, the response changes with distance are essentially eliminated.

2.6.6. *Legendre-shaded CBT circular-arc array*

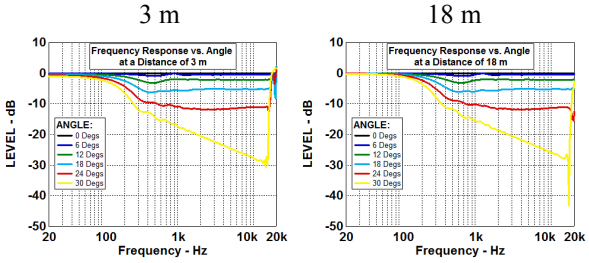

Fig. 28. Off-axis frequency responses of the shaded circular-arc line array at distances of 3 m (left) and 18 m (right).

The off-axis frequency response curves of the Legendre-shaded circular-arc array are nearly perfect out to about – 12 dB down from on axis. Beyond this angle, the response drops with frequency. Hardly any ripple exists in the responses. In addition, the response changes with distance are essentially nonexistent.

2.6.7. *Legendre-shaded delay-curved CBT straight-line array*

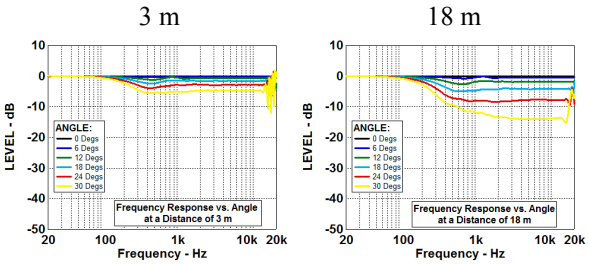

Fig. 29. Off-axis frequency responses of the shaded delay-curved CBT straight-line array at distances of 3 m (left) and 18 m (right).

As with the shaded circular-arc array, the off-axis frequency response curves of the Legendre-shaded delay-curved straight-line array are extremely good. Although the off-axis response curves are very flat and ripple free, there is still variation with distance. The frequency response levels drop off more quickly at the farthest distance, i.e. the array is more directional as distance increases.

2.6.8. *Off-axis frequency response uniformity ranking scores:*

The following list shows the subjective scores I assigned to each array for off-axis frequency response curve uniformity, on a scale from 1 to 10.

1. Un-shaded straight-line array: 1
2. Hann-shaded straight-line array: 2
3. Un-shaded "J"-line array: 1
4. Un-shaded spiral- or progressive-line array: 3
5. Un-shaded circular-arc array: 8
6. Legendre-shaded CBT circular-arc array: 10
7. Legendre-shaded delay-curved CBT straight-line array: 9

2.6.9. *Array ranking for frequency response uniformity:*

The following list orders the arrays in rank order according to their off-axis frequency response curve uniformity scores with the highest ranked array on top.

1. Legendre-shaded CBT circular-arc array: 10
2. Legendre-shaded delay-curved CBT straight-line array: 9
3. Un-shaded circular-arc array: 8
4. Un-shaded spiral- or progressive-line array: 3
5. Hann-shaded straight-line array: 2
6. Un-shaded "J"-line array: 1
7. Un-shaded straight-line array: 1

Here the CBT and the un-shaded circular-arc arrays are on top, with the rest of the arrays on the bottom.

2.7. Sound Pressure Level vs. Distance:

The sound pressure level (SPL) versus distance of the arrays was evaluated at octave frequencies of 62.5 Hz to 8 kHz. The SPL vs. distance was evaluated at two different array launch heights: a) the center of the array and b) the top of the array.

Loudspeaker line arrays exhibit two distinct regions of sound pressure rolloff with distance depending on the closeness of the array. Close to the array in the near-field, the SPL rolls off about at 3 dB per doubling of distance. At farther distances, the rolloff approaches 6 dB per doubling of distance.

Unfortunately, the rolloff is strongly a function of frequency. If the SPL rolloff versus distance at specific frequencies is even and consistent, the frequency response at the different distances will be flat or can be made flat with equalization at a specific distance.

The following graphs plot the SPL vs. distance at nine octave frequencies from 32 Hz to 8 kHz plotted on a log distance scale covering a four decade range of 25 mm to 250 m (1" to 10,000"). Each draw-away curve is color coded with the following colors:

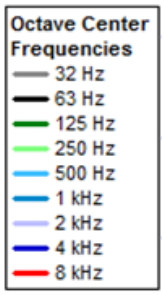

The SPL rolloff with distance was simulated for two different launch points on the array: a) from the center (midpoint), and b) from the top (endpoint). This was

done because previous authors have noted that the SPL vs. distance changes significantly depending on the draw-away point on the array [7, Section 2.5.2].

In all cases, the SPL rolloff was calculated on a path normal to the source assuming a straight-line array. For the simulations in this paper with the arrays facing the right, this means that the rolloff was calculated on a draw-away line proceeding to the right.

For reference, all graphs show dashed slope lines indicating 3 dB and 6 dB per doubling of distance.

2.7.1. *Un-shaded straight-line array*

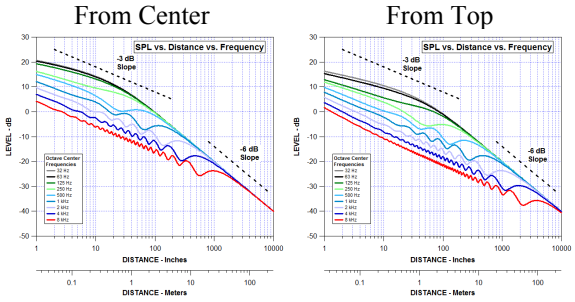

Fig. 30. SPL vs. Distance for the un-shaded straight-line array with trajectories starting at the center (left) and top (right).

As with all the following SPL rolloff plots, the SPL vs. distance plot of the un-shaded straight-line array exhibits a characteristic rolloff of approximate 3 dB per doubling of distance near the array (out to about 1 to 10 m depending on frequency) and 6 dB per doubling of distance at farther distances. The details of the rolloff in the two different regions change depending on the array type.

In general for the un-shaded straight-line array, the rolloff is strongly frequency dependent in the 3 dB rolloff region and well-behaved beyond. Near the array, the rolloff exhibits much ripple and variation with frequency, with the higher frequencies rolling off sooner and the 3 dB rolloff extending out farther in distance. If the SPL rolloff is calculated from the top of the array, the 3 dB region extends farther out in distance with essentially the same rolloff characteristics as the center rolloff.

2.7.2. *Hann-shaded straight-line array*

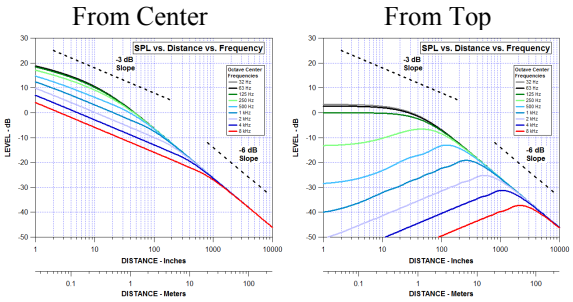

Fig. 31. SPL vs. Distance for the Hann-shaded straight-line array with trajectories starting at the center (left) and top (right).

Here there is a dramatic difference in the curves comparing the center launch point (left) versus the top launch point (right). All curves are very smooth with absolutely no ripple but the top launch point data is very sensitive to the dramatic narrowing of the polar pattern with frequency.

The top launch point is effectively very far off-axis of the array for distances close to the array. This causes the extreme attenuation of the of the SPL vs. Distance curves for the higher frequencies near the array. At points far from the array, all the draw-away-lines converge.

2.7.3. *Un-shaded "J"-line array*

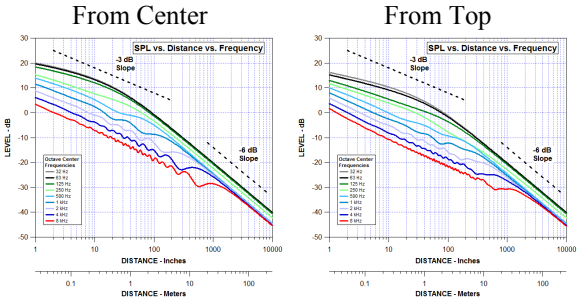

Fig. 32. SPL vs. Distance for the un-shaded "J"-line array with trajectories starting at the center (left) and top (right).

The SPL rolloff of the un-shaded "J"-line array is very similar to the SPL rolloff of the un-shaded straight-line array except that the far-field rolloff is frequency dependent. Refer to the previous comments on the un-shaded straight-line array.

2.7.4. *Un-shaded spiral-line array*

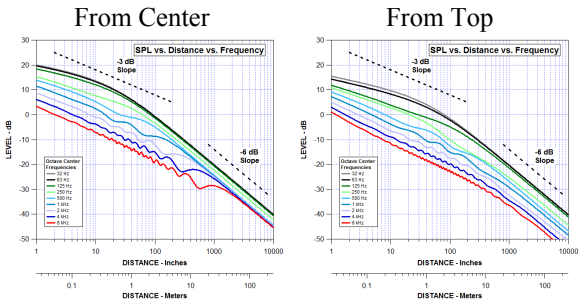

Fig. 33. SPL vs. Distance for the un-shaded spiral-line array with trajectories starting at the center (left) and top (right).

From the center, the SPL vs. distance characteristics of the un-shaded spiral-line array is essentially the same as the previous "J"-line array. However, the rolloff from the top is much more uniform than all the previous arrays. It exhibits excellent uniformity with frequency and much less ripple, but also exhibits frequency dependent lowering of the draw-away lines as frequency increases.

2.7.5. *Un-shaded circular-arc line array*

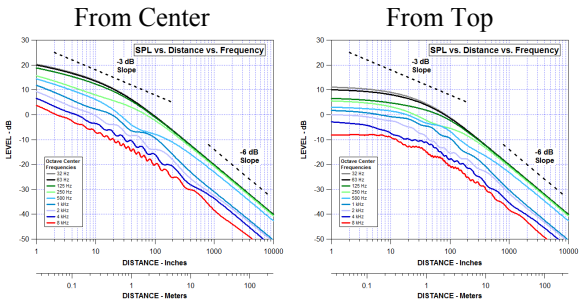

Fig. 34. SPL vs. Distance for the un-shaded circular-arc line array with trajectories starting at the center (left) and top (right).

The SPL rolloff of the un-shaded circular-arc line array is the most uniform of all the arrays considered so far except for some ripple in the rolloff. Interestingly, the SPL rolloff from the top of the array (right) exhibits a plateau region near the array where the SPL stays approximately constant out to about 2 to 3 m in front of the array.

2.7.6. *Legendre-shaded CBT circular-arc array*

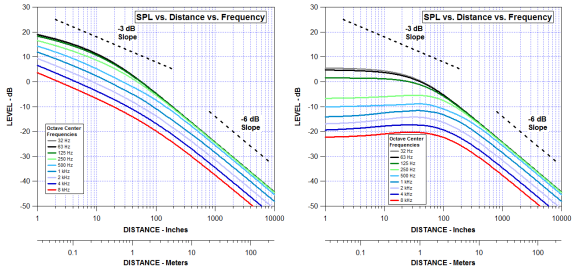

Fig. 35. SPL vs. Distance for the shaded circular-arc line array with trajectories starting at the center (left) and top (right).

The SPL rolloff of the Legendre-shaded circular-arc line array is extremely uniform with both frequency and distance. The uniformity of the rolloff trajectories means that the frequency response at different distances from this array will be very uniform and well behaved. In addition, the rolloff emanating from the top of the array (right), exhibits a plateau region where the SPL is quite constant with distance out to about 3 m in front of the array.

2.7.7. *Legendre-shaded delay-curved CBT straight-line array*

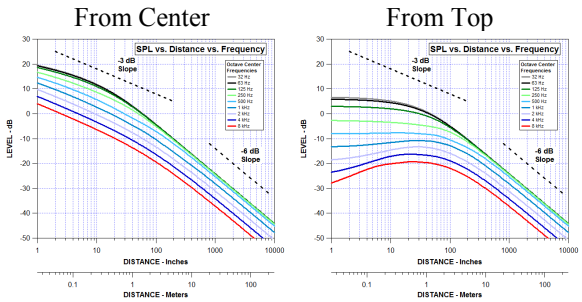

Fig. 36. SPL vs. Distance for the shaded delay-curved straight-line array with trajectories starting at the center (left) and top (right).

The Legendre-shaded delay-curved straight-line array's rolloff with distance is also very uniform and well behaved and is an excellent approximation of the SPL vs. Distance performance of the previous circular-arc version of the CBT array.

2.7.8. SPL vs. Distance uniformity ranking scores:

The following list shows the subjective scores I assigned to each array for the SPL vs. Distance uniformity, on a scale from 1 to 10.

1. Un-shaded straight-line array: 2
2. Hann-shaded straight-line array: 1
3. Un-shaded "J"-line array: 3
4. Un-shaded spiral- or progressive-line array: 5
5. Un-shaded circular-arc array: 8
6. Legendre-shaded CBT circular-arc array: 10
7. Legendre-shaded delay-curved CBT straight-line array: 9

2.7.9. Array ranking for SPL vs. Distance uniformity:

The following list orders the arrays in rank order according to their SPL vs. Distance uniformity scores with the highest ranked array on top.

1. Legendre-shaded CBT circular-arc array: 10
2. Legendre-shaded delay-curved CBT straight-line array: 9
3. Un-shaded circular-arc array: 8
4. Un-shaded spiral-line array: 5
5. Un-shaded "J"-line array: 3
6. Un-shaded straight-line array: 2
7. Hann-shaded straight-line array: 1

Here both CBT arrays are on top, and as before, the shaded and un-shaded straight-line arrays are on the bottom.

2.8. Near-far polar pattern uniformity:

The polar pattern of the array was evaluated for its uniformity with distance. The following graphs show polar pattern shapes and beamwidth vs. frequency data at three distances from the array: 2 m, 6 m, and 18 m. Two sets of polars are shown for the three distances at 800 Hz and 8 kHz. This information yields a reasonable estimate of the changes in the polar patterns with distance.

The following sets of data are plotted for each of the arrays. Brief comments follow each array type.

2.8.1. Un-shaded straight-line array

Polars at 800 Hz:

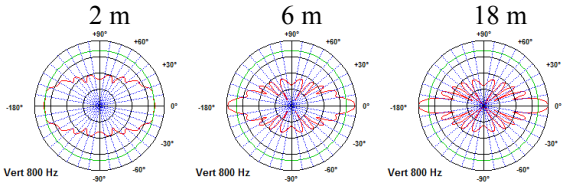

Polars at 8 kHz:

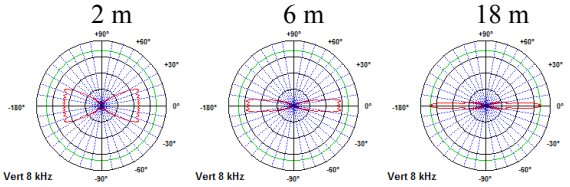

Beamwidth vs. Frequency:

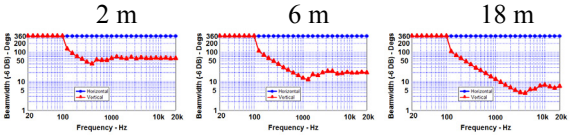

Fig. 37. Polar and beamwidth data for the un-shaded straight-line array at distances of 2 m (left), 6 m (middle), and 18 m (right). Polars at 800 Hz (top), 8 kHz (middle), and beamwidth (bottom).

The polar patterns of the un-shaded straight-line array are a strong function of distance and frequency, i.e. the polar pattern continually narrows with frequency and changes significantly with distance. The beamwidth vs. frequency data clearly shows this variation.

2.8.2. Hann-shaded straight-line array

Polars at 800 Hz:

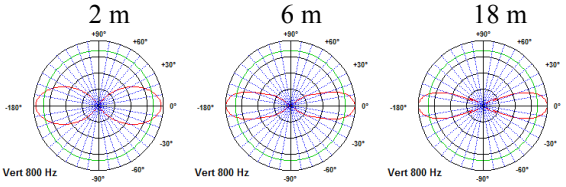

Polars at 8 kHz:

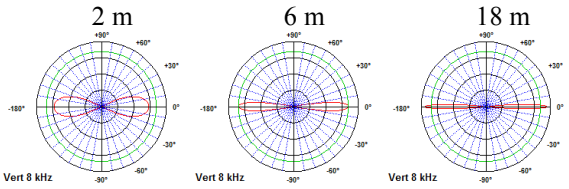

Beamwidth vs. Frequency:

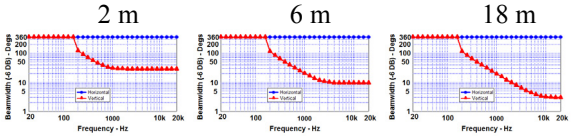

Fig. 38. Polar and beamwidth data for the Hann-shaded straight-line array at distances of 2 m (left), 6 m (middle), and 18 m (right). Polars at 800 Hz (top), 8 kHz (middle), and beamwidth (bottom).

The polars and beamwidth of the Hann-shaded straight-line array are much superior to the un-shaded straight-line array but still change strongly with distance and frequency.

2.8.3. Un-shaded "J"-line array

Polars at 800 Hz:

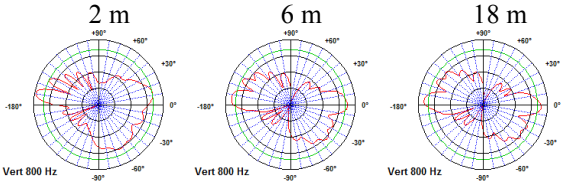

Polars at 8 kHz:

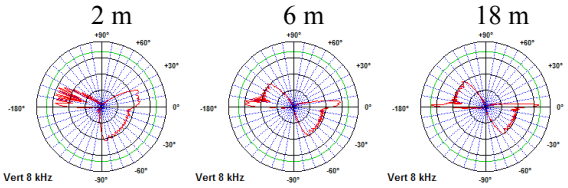

Beamwidth vs. Frequency:

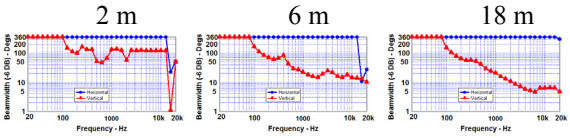

Fig. 39. Polar and beamwidth data for the un-shaded "J"-line array at distances of 2 m (left), 6 m (middle), and 18 m (right). Polars at 800 Hz (top), 8 kHz (middle), and beamwidth (bottom).

The polars of the un-shaded "J"-line array change with frequency but not nearly as strongly as the un-shaded and shaded straight-line arrays. The beamwidth data still shows significant change with distance getting narrower with frequency.

2.8.4. Un-shaded spiral-line array

Polars at 800 Hz:

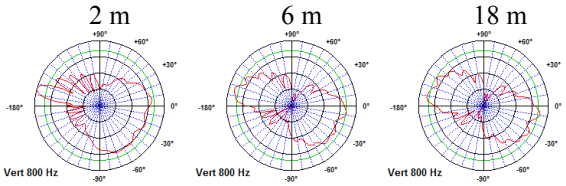

Polars at 8 kHz:

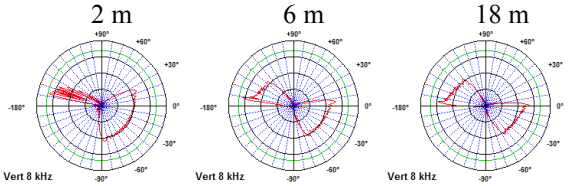

Beamwidth vs. Frequency:

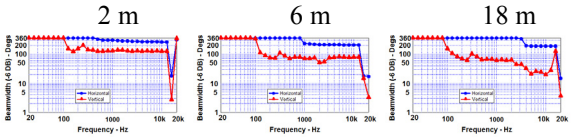

Fig. 40. Polar and beamwidth data for the un-shaded spiral-line array at distances of 2 m (left), 6 m (middle), and 18 m (right). Polars at 800 Hz (top), 8 kHz (middle), and beamwidth (bottom).

The polars and beamwidth data for the un-shaded spiral-line array are much more uniform with distance than the previous arrays.

2.8.5. Un-shaded circular-arc line array

Polars at 800 Hz:

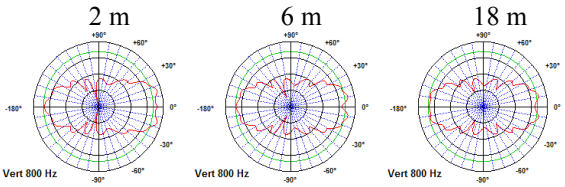

Polars at 8 kHz:

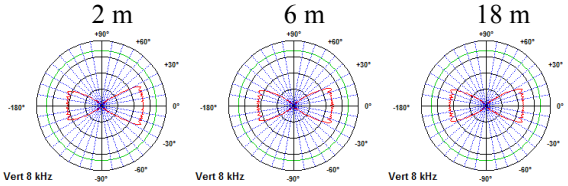

Beamwidth vs. Frequency:

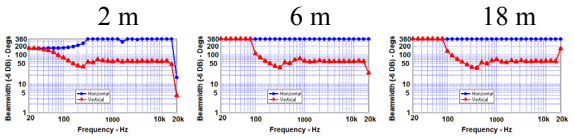

Fig. 41. Polar and beamwidth data for the un-shaded circular-arc line array at distances of 2 m (left), 6 m (middle), and 18 m (right). Polars at 800 Hz (top), 8 kHz (middle), and beamwidth (bottom).

The un-shaded circular-arc line array's polars and beamwidth data has much less variation with distance than even the previous un-shaded spiral-line array's data.

2.8.6. Legendre-shaded CBT circular-arc line array

Two sets of data are shown here. The first is generated by rotating the array around its center of curvature, and the second by rotating around the front of the array.

Rotate around center of curvature:

Polars at 800 Hz:

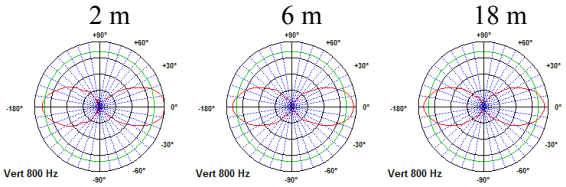

Polars at 8 kHz:

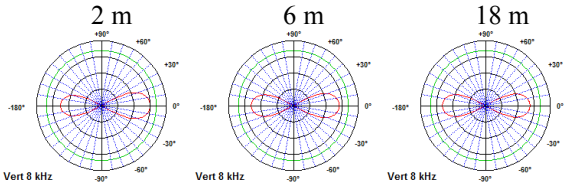

Beamwidth vs. Frequency:

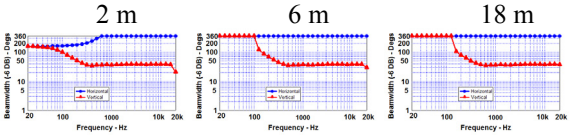

Fig. 42. Polar and beamwidth data for the shaded circular-arc line array at distances of 2 m (left), 6 m (middle), and 18 m (right). Polars at 800 Hz (top), 8 kHz (middle), and beamwidth (bottom). This set of data was generated by rotating the array around its center of curvature.

The polar and beamwidth data for the Legendre-shaded circular-arc line array are extremely uniform with distance when the data is gathered by rotating the array around its circular-arc center of curvature. To investigate the effect of rotating the array around its actual center (or front), rather than the center of curvature, the following polars were generated by rotating around the center or front of the array.

Rotate around front of array:
Polars at 800 Hz:

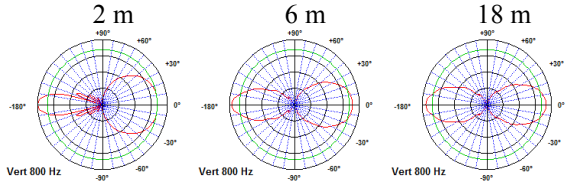

Polars at 8 kHz:

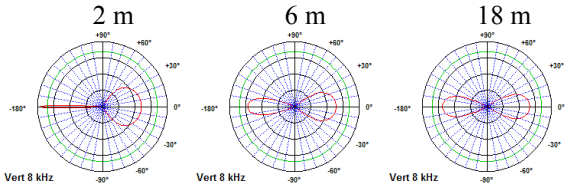

Beamwidth vs. Frequency:

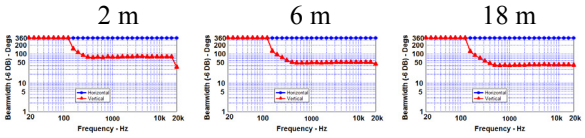

Fig. 43. Polar and beamwidth data for the shaded circular-arc line array at distances of 2 m (left), 6 m (middle), and 18 m (right). Polars at 800 Hz (top), 8 kHz (middle) , and beamwidth (bottom). This set of data was generated by rotating the array around the array's center (front).

These polars which were run by rotating the array around the center or front of the array are equally as smooth and well behaved as the ones rotated around the array's center of curvature. However, the data shows that the polar shapes and beamwidth change as a function of distance, particularly near the array. This data clearly shows the superiority of rotating the circular-arc array around its center of curvature, rather than its physical center or front, to regularize polar changes with distance.

2.8.7. Legendre-shaded delay-curved CBT straight-line array

Polars at 800 Hz:

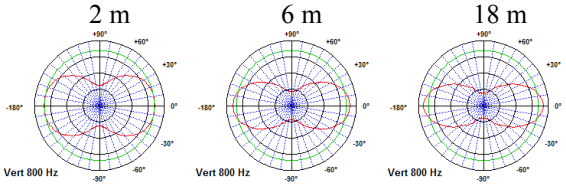

Polars at 8 kHz:

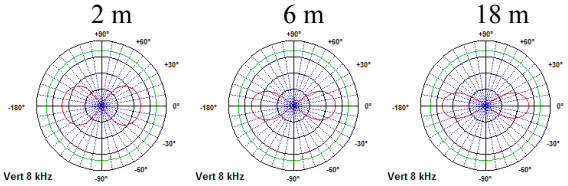

Beamwidth vs. Frequency:

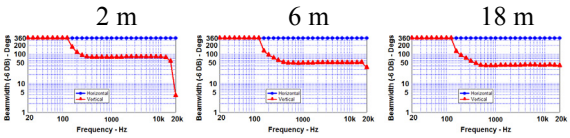

Fig. 44. Polar and beamwidth data for the shaded delay-curved straight-line array at distances of 2 m (left), 6 m (middle), and 18 m (right). Polars at 800 Hz (top), 8 kHz (middle), and beamwidth (bottom).

The polars and beamwidth data for the Legendre-shaded delay-curved straight-line array are equally as smooth and well behaved as the Legendre-shaded circular-arc line array but exhibit some changes with distance particularly for locations close to the array.

2.8.8. Near-far polar pattern uniformity ranking scores:

The following shows the subjective scores I assigned to each array for the near-far polar pattern uniformity, on a scale from 1 to 10.

1. Un-shaded straight-line array: 1
2. Hann-shaded straight-line array: 2
3. Un-shaded "J"-line array: 4
4. Un-shaded spiral-line array: 7

5. Un-shaded circular-arc array: 8
6. Legendre-shaded CBT circular-arc array: 10
7. Legendre-shaded delay-curved CBT straight-line array: 9

2.8.9. Array ranking for near-far polar pattern uniformity:

The following lists the arrays in rank order according to their near-far polar pattern uniformity with the highest ranked array on top.

1. Legendre-shaded CBT circular-arc array: 10
2. Legendre-shaded delay-curved CBT straight-line array: 9
3. Un-shaded circular-arc array: 8
4. Un-shaded spiral- or progressive-line array: 7
5. Un-shaded "J"-line array: 4
6. Hann-shaded straight-line array: 2
7. Un-shaded straight-line array: 1

Here the CBT and the un-shaded circular-arc arrays are on top, the spiral- and "J"-line arrays in the middle, and the rest of the arrays on the bottom.

2.9. Array Horizontal Responses:

Although this paper considered only vertical polar information, some horizontal polar data was generated for comparison purposes. Section 8 Appendix 3 shows the array's far-field (250 m) horizontal polar responses at three different frequencies of 1.25, 4, and 12.5 kHz These polars are shown here for information only and were not used to rank the arrays.

Note that all the straight line arrays have omnidirectional horizontal polar responses. This is in contrast with the non-straight remaining arrays, which exhibit a pointed maximum in the polar response at ±90° with a reduced level on axis that is frequency dependent. This behavior was pointed out for the circular-arc arrays in [10].

3. ANALYSIS RESULTS AND RANKING

Section 9 Table 4 tabulates the results of this analysis summing the individual scores for each array and performance parameter. This tabulation yielded the following ranking of the seven arrays with the CBT circular-arc array on top and the un-shaded straight-line array on the bottom:

1. CBT circular-arc array,
2. CBT delay-curved straight-line array,
3. Un-shaded circular-arc array,
4. Spiral-line array,
5. "J"-line array,
6. Straight-line array (Hann shaded),
7. Straight-line array (not shaded).

4. SUMMARY

This paper presented performance simulation data that allowed several different types of loudspeaker line arrays to be compared and ranked. The following types of arrays were ranked:

1. An un-shaded straight-line array,
2. A Hann-shaded straight-line array,
3. An un-shaded "J"-line array with straight top half and circular-arc bottom half ,
4. An un-shaded spiral- or progressive-line array,
5. An un-shaded circular-arc array,
6. A Legendre-shaded CBT circular-arc array, and
7. A Legendre-shaded delay-curved CBT straight-line array.

Simulated performance data presented included:

1) Beamwidth vs. frequency data plotted at several different distances,
2) Far field directivity vs. frequency,
3) Vertical sound-field data plotted in a 6m x 6m region vs. frequency,
4) Polar data plotted at several distances and frequencies,
5) Array off-axis frequency responses plotted at two different distances, and
6) Sound pressure rolloff versus frequency and distance data plotted with trajectories that originate from the center and top of the array.

The performance data for all the arrays was subjectively ranked for each performance type on a scale from 1 to 10 and then totaled (scale 8 to 80) for each array, to yield the final array ranking:

1. CBT circular-arc array: 80,
2. CBT delay-curved straight-line array: 77,
3. Un-shaded circular-arc array: 54,
4. Spiral-line array: 46,
5. "J"-line array: 26,
6. Straight-line array (Hann shaded): 23, and
7. Straight-line array (not shaded): 10

The performance data clearly shows the superiority of the shaded circular-arc CBT and shaded delay-curved CBT arrays. All the performance data for these two arrays was extremely uniform and well behaved. The Legendre-shaded circular-arc CBT array is clearly the winner here because of its uniformity of coverage and the independence of its performance with distance. The performance of the delay-curved straight-line CBT array is also very uniform and well behaved and nearly matches the performance of the circular-arc CBT array.

A distant third to the CBT arrays is the spiral-line array with the remaining "J"-line and straight-line arrays holding up the bottom of the rankings.

5. REFERENCES

[1] "Huygens–Fresnel Principle," From Wikipedia, the free encyclopedia, (http://en.wikipedia.org/wiki/Huygens%E2%80%93Fresnel_principle).

[2] D. B. Keele, Jr., "The Application of Broadband Constant Beamwidth Transducer (CBT) Theory to Loudspeaker Arrays," 109th Convention of the Audio Engineering Society, Convention paper 5216 (Sept. 2000).

[3] D. L. Smith, "Discrete-Element Line Arrays--Their Modeling and Optimization," J. Audio Eng. Soc., p. 949, vol. 45, no.11 (November 1997).

[4] S. Ureda, "Line Arrays: Theory and Applications," 110th Convention of the Audio Engineering Society, Convention paper 5304 (June 2001).

[5] G. L. Augspurger, "Near-Field and Far-Field Performance of Large Woofer Arrays," J. Audio Eng. Soc., p. 231, vol.38, no.4 (April 1990).

[6] M. S. Ureda, "'J' and Spiral Line Arrays," 111th Convention of the Audio Engineering Society, Convention paper 5485 (Sept. 2001).

[7] M. S. Ureda, "Analysis of Loudspeaker Line Arrays," J. Audio Eng. Soc., vol. 52, no. 5 (May 2004).

[8] P. H. Rogers, and A. L. Van Buren, "New Approach to a Constant Beamwidth Transducer," J. Acous. Soc. Am., vol. 64, no. 1, pp. 38-43 (July 1978).

[9] D. B. Keele, Jr., "Implementation of Straight-Line and Flat-Panel Constant Beamwidth Transducer (CBT) Loudspeaker Arrays Using Signal Delays," 113th Convention of the Audio Engineering Society, Convention paper 5653 (Oct. 2002).

[10] D. B. Keele, Jr., "The Full-Sphere Sound Field of Constant Beamwidth Transducer (CBT) Loudspeaker Line Arrays," J. Aud. Eng. Soc., vol. 51, no. 7/8., pp. 611-624 (July/August 2003).

[11] D. B. Keele, Jr., "Practical Implementation of Constant Beamwidth Transducer (CBT) Loudspeaker Circular-Arc Line Arrays," presented at the 115th Convention of the Audio Engineering Society, New York, Convention paper 5863 (Oct. 2003).

[12] D. B. Keele, Jr. and D. J. Button, "Ground-Plane Constant Beamwidth Transducer (CBT) Loudspeaker Circular-Arc Line Arrays." presented at the 119th Convention of the Audio Engineering Society, Convention paper 6594 (Oct. 2005).

[13] "Side Lobe," From Wikipedia, the free encyclopedia, (http://en.wikipedia.org/wiki/Side_lobe). Quote from this article: "…. in which the element spacing is much greater than a half wavelength, the aliasing effect causes some sidelobes to become substantially larger in amplitude, and approaching the level of the main lobe; these are called *grating lobes*, and they are identical, or nearly identical…."

6. APPENDIX 1: ARRAY SOUND-FIELD DISPLAYS

The following are generated at octaves from 125 Hz to 16 kHz.

6.1. Un-shaded straight-line array:

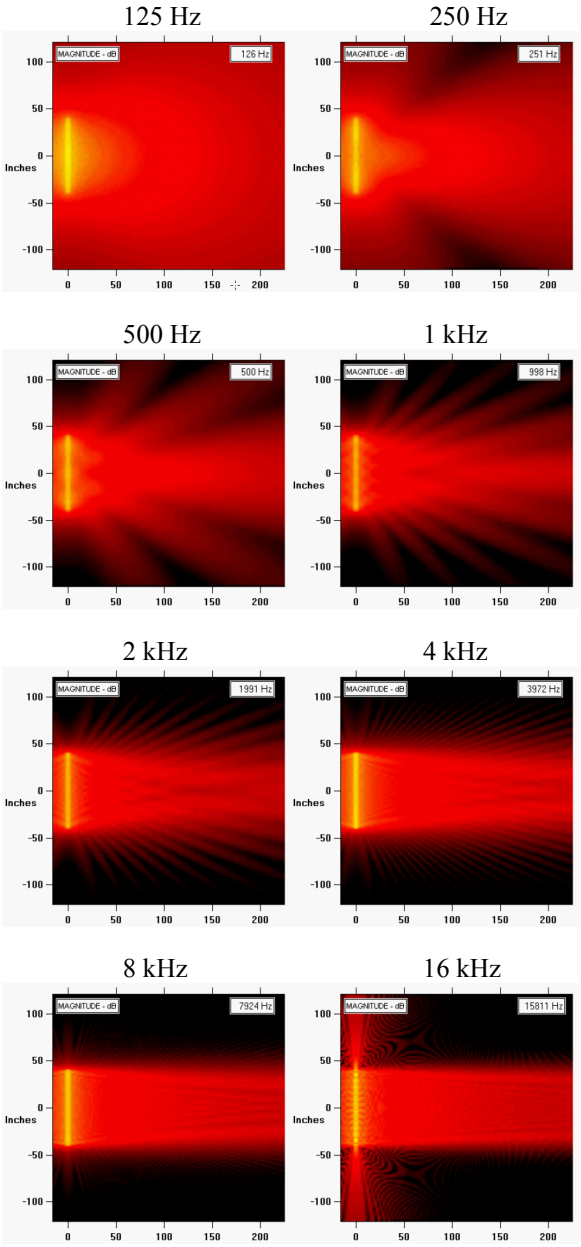

6.2. Hann-shaded straight-line array:

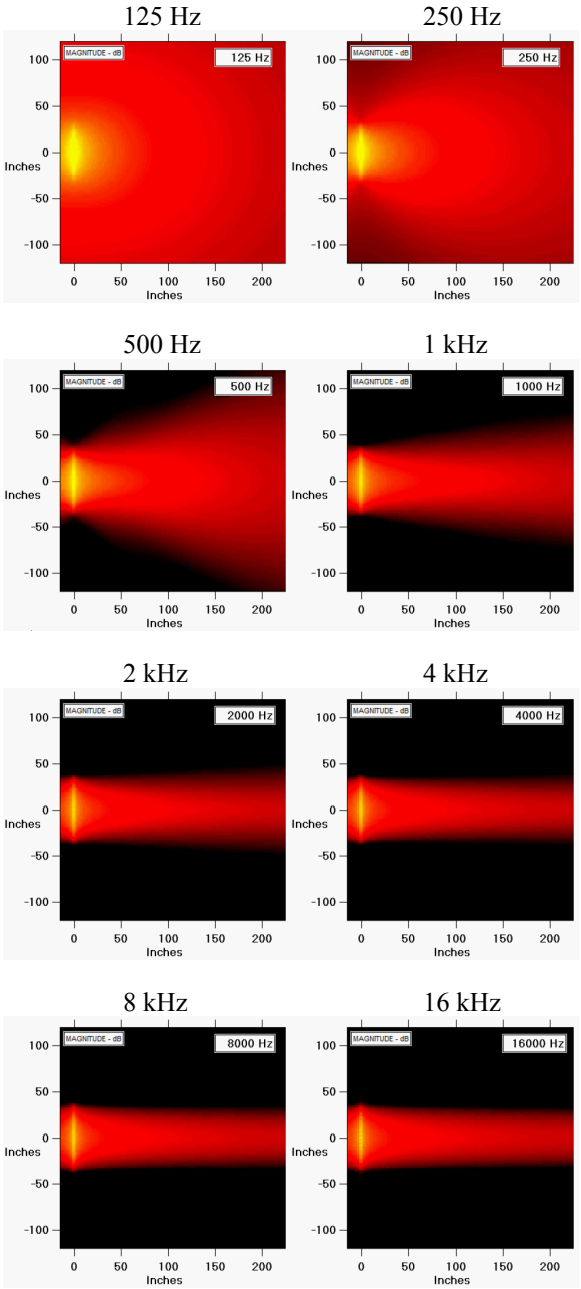

6.3. Un-shaded "J"-line array:

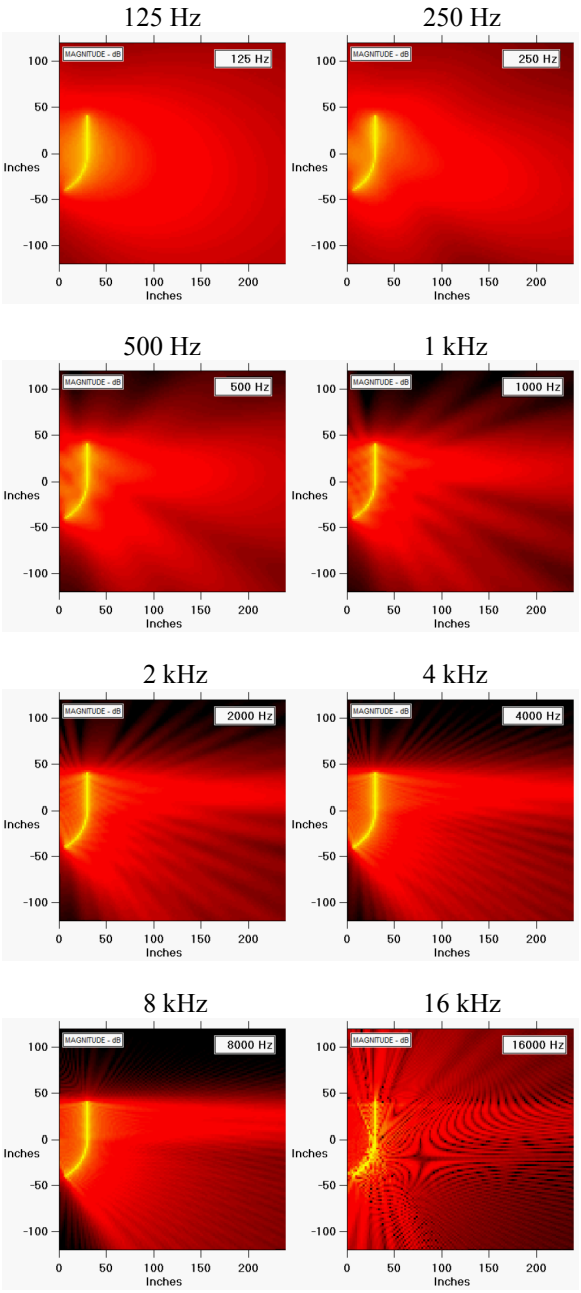

6.4. Un-shaded spiral-line array:

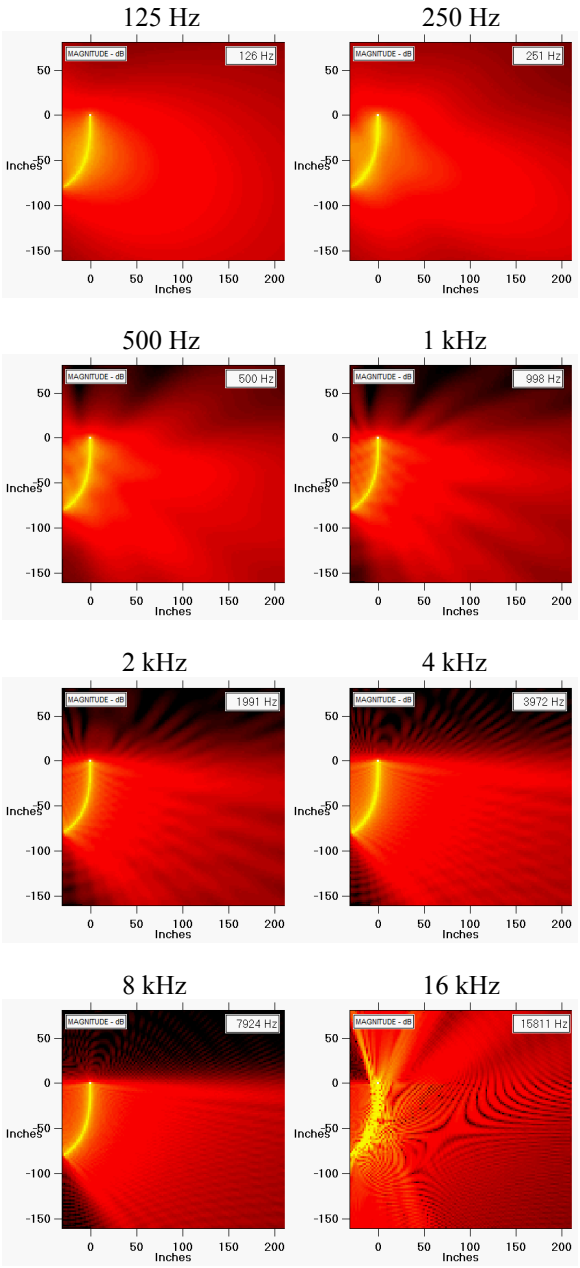

6.5. Un-shaded circular-arc array:

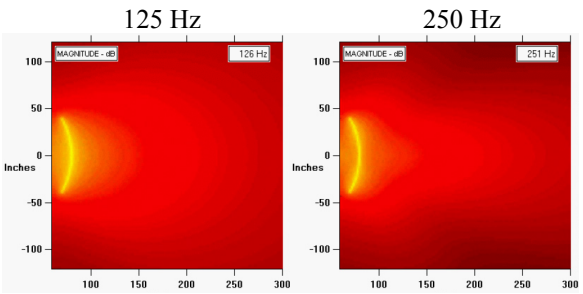

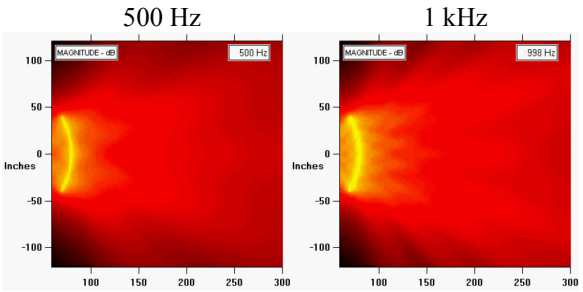

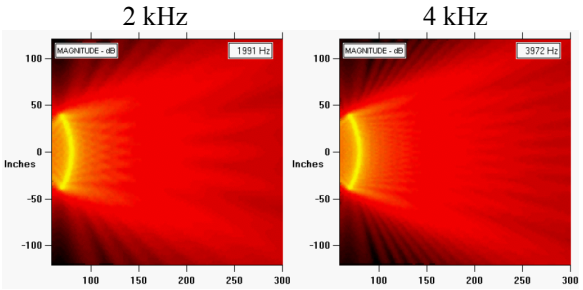

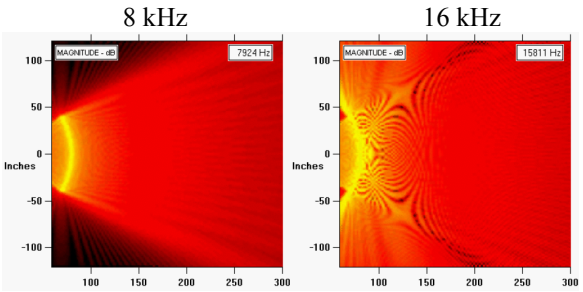

6.6. Legendre-shaded CBT circular-arc array:

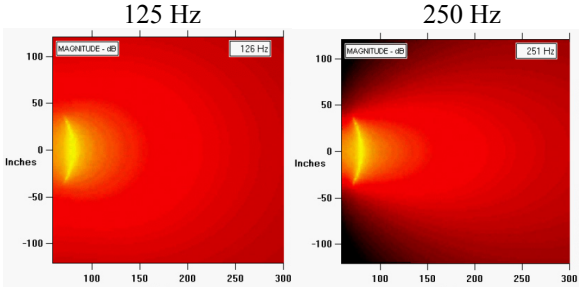

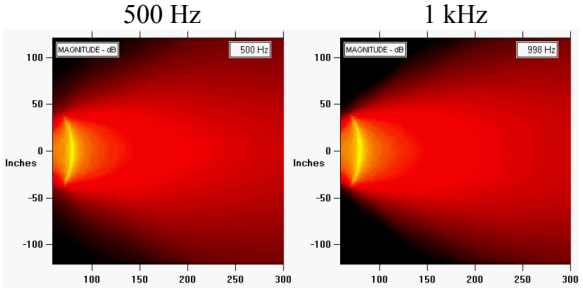

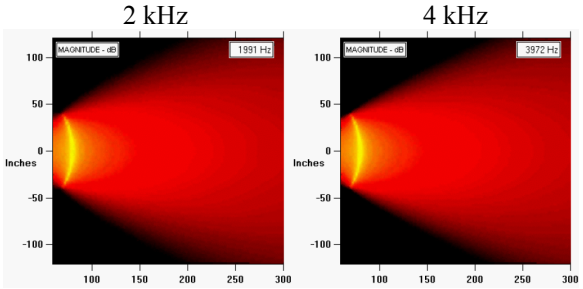

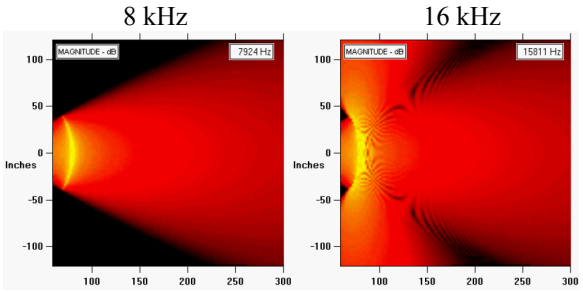

6.7. Legendre-shaded delay-curved CBT straight-line array:

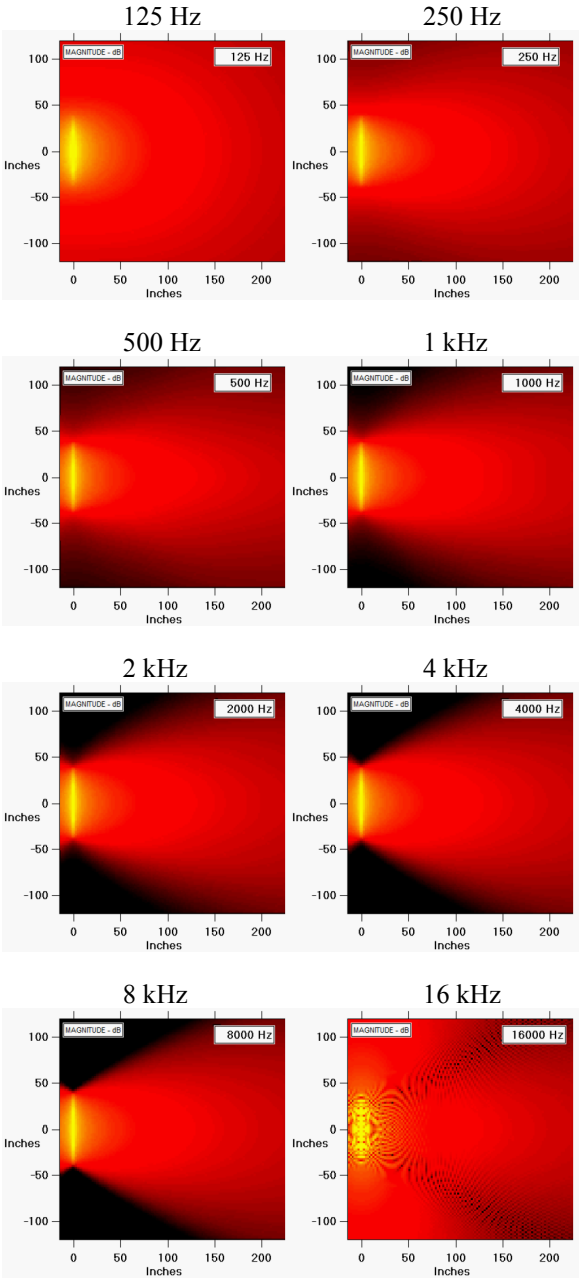

7. APPENDIX 2: ARRAY VERTICAL POLAR RESPONSE

The following polars were generated for each array at octave frequencies from 125 Hz to 16 kHz. All the arrays were rotated about the center of the array except for the circular-arc arrays which were rotated about the center of curvature of the array. The polars were generated at an equivalent far-field distance of 250 m.

The polars cover a range of 40 dB with 0 dB on the outside edge and -40 dB in the center. 10 dB per major division. A green circle indicates the -6 dB down level. The polars have not been normalized to the on axis level, and preserve any attenuation inherent to the configuration of a specific array.

This space intentionally kept empty.

Un-shaded straight-line array:

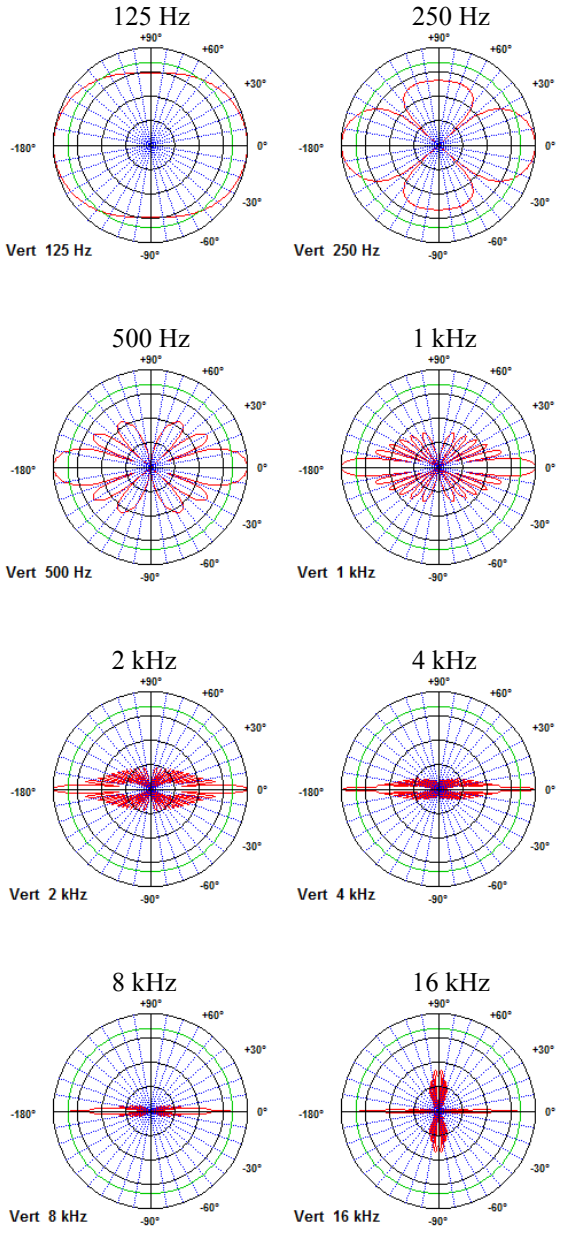

7.1. Hann-shaded straight-line array:

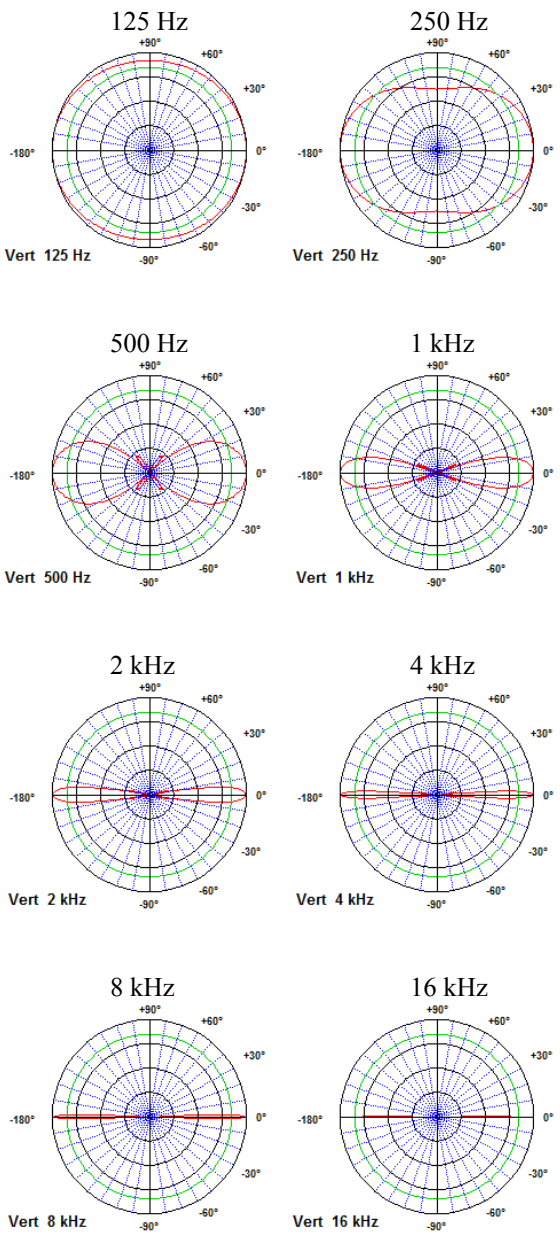

7.2. Un-shaded "J"-line array:

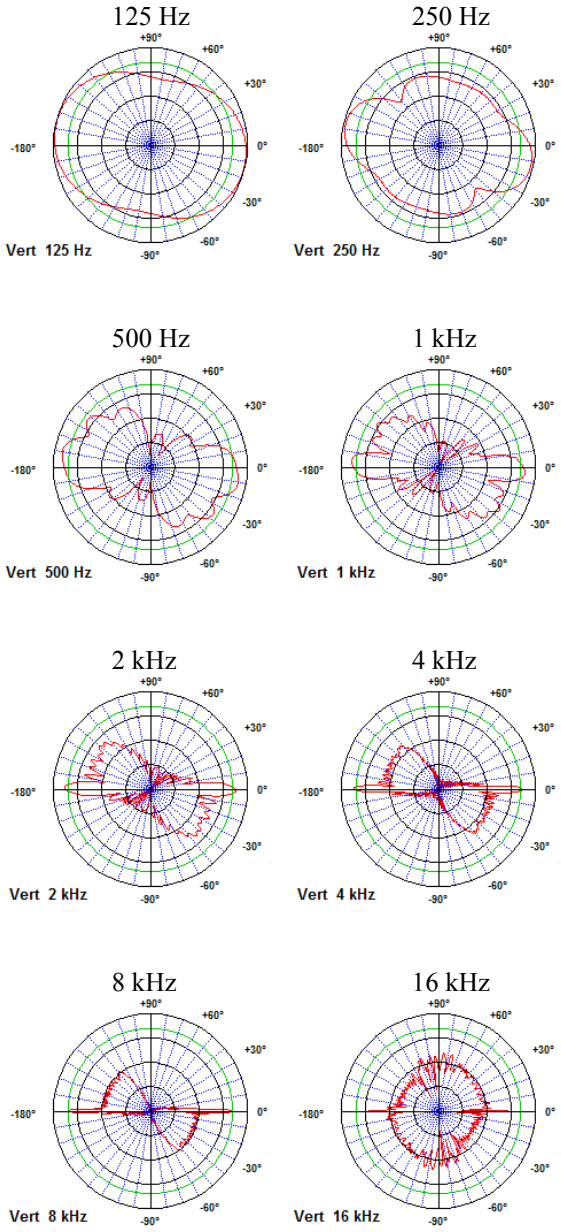

7.3. Un-shaded spiral-line array:

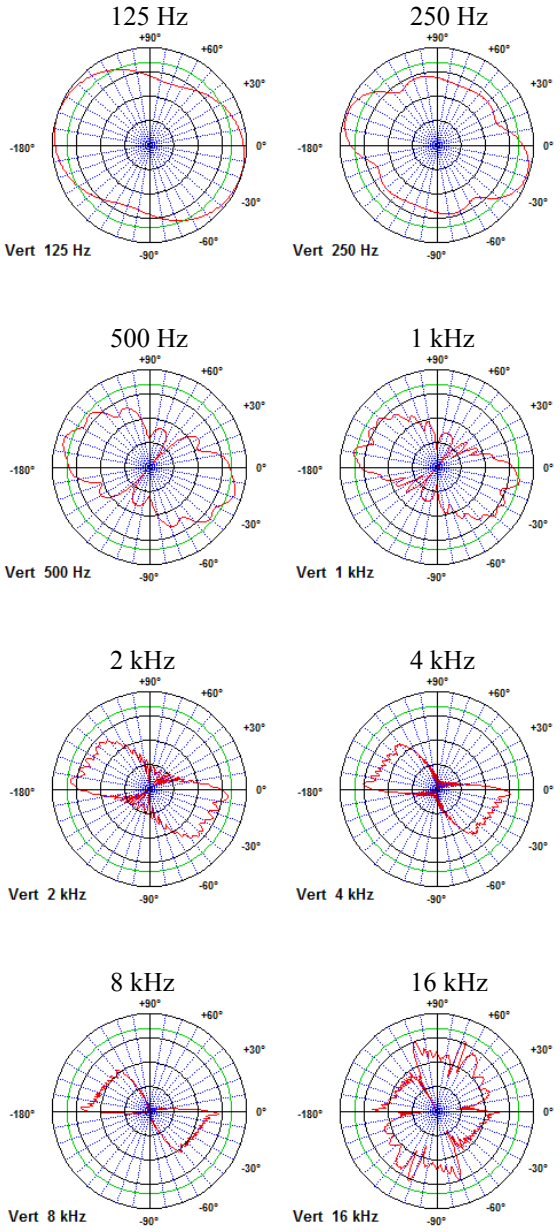

7.4. Un-shaded circular-arc array:

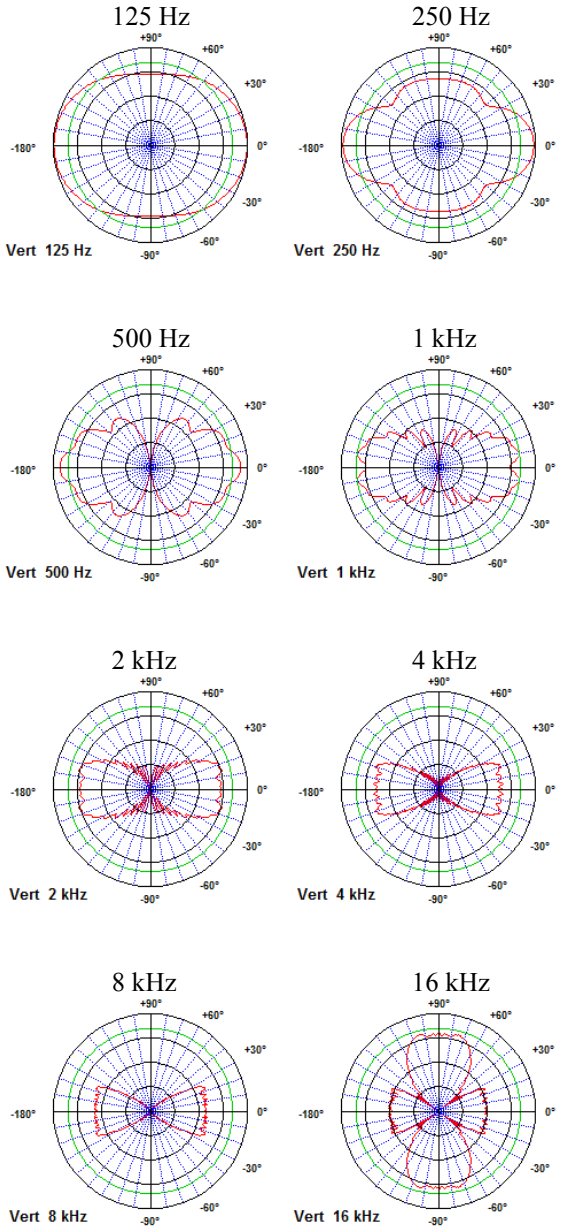

7.5. Legendre-shaded CBT circular-arc array:

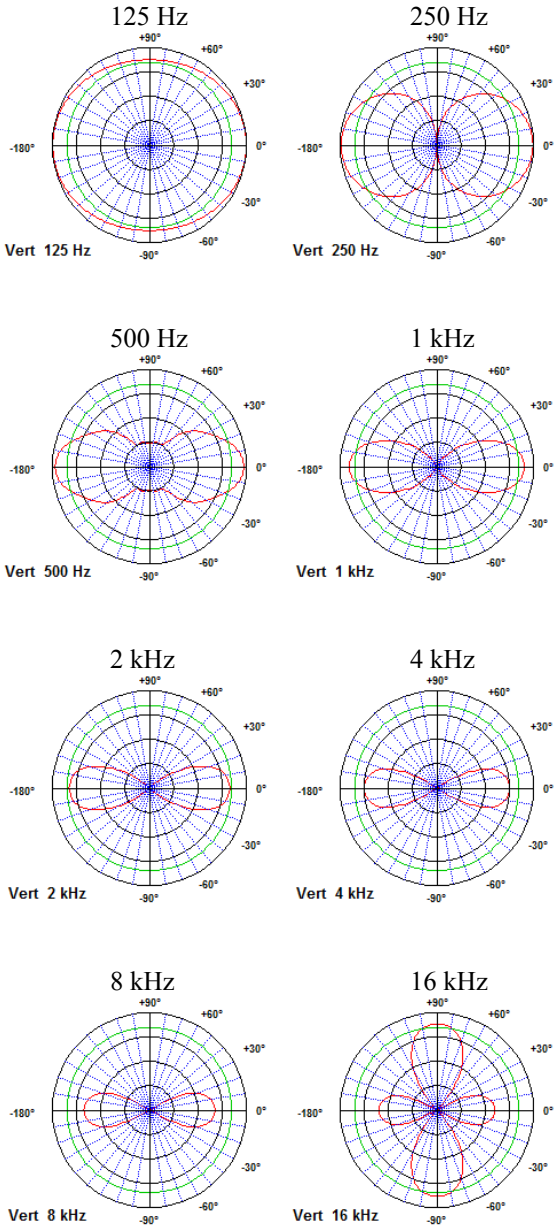

7.6. Legendre-shaded delay-curved CBT straight-line array:

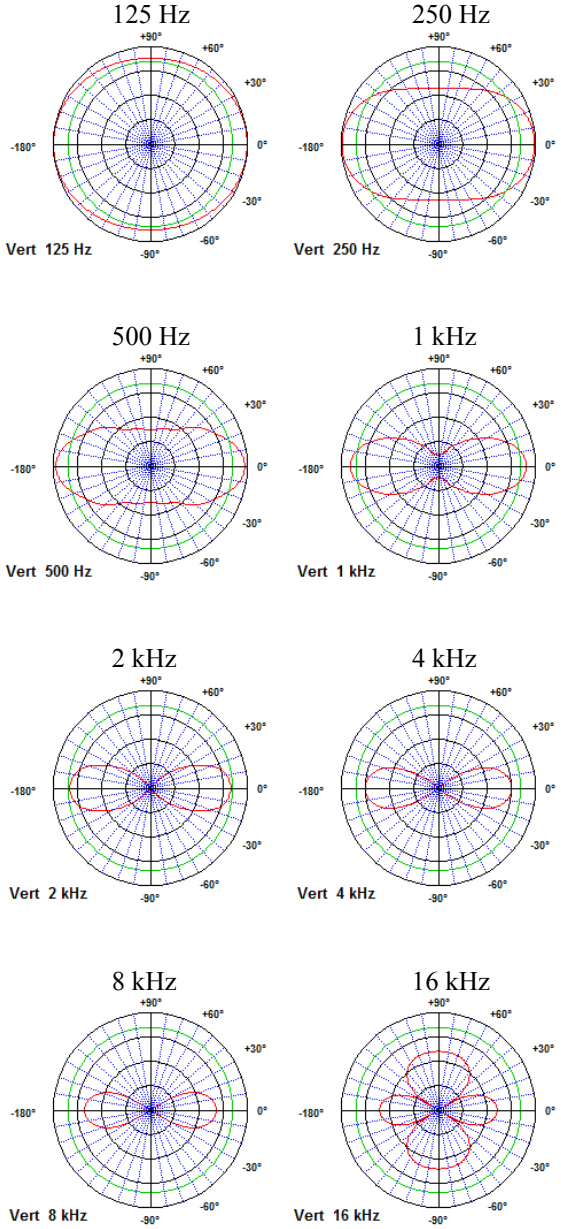

8. APPENDIX 3: ARRAY HORIZONTAL POLAR RESPONSE

This appendix shows the far field (250 m) horizontal polar responses at three different frequencies of 1.25, 4, and 12.5 kHz. These polars are shown here for information only and were not used to rank the arrays. Note that all the straight line arrays have omnidirectional horizontal polar responses. This is in contrast with the non-straight remaining arrays, which exhibit a maximum in the polar response at ±90° and a reduced frequency-dependent level on axis.

8.1. Un-shaded straight-line array:

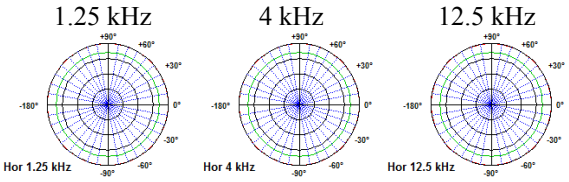

8.2. Hann-shaded straight-line array:

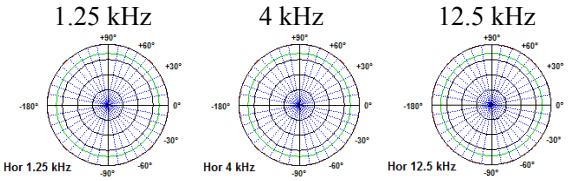

8.3. Un-shaded “J”-line array:

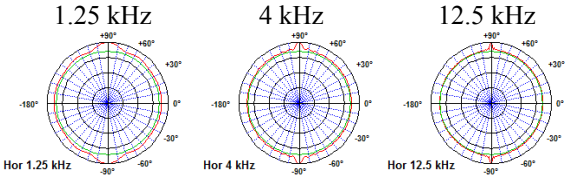

8.4. Un-shaded spiral-line array:

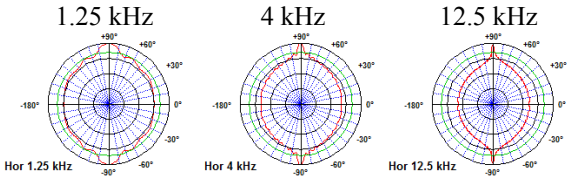

8.5. Un-shaded circular-arc array:

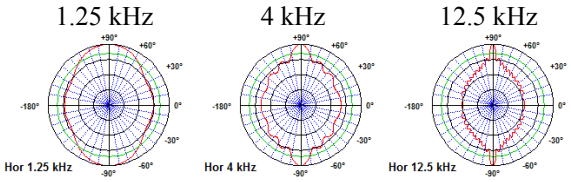

8.6. Legendre-shaded CBT circular-arc array:

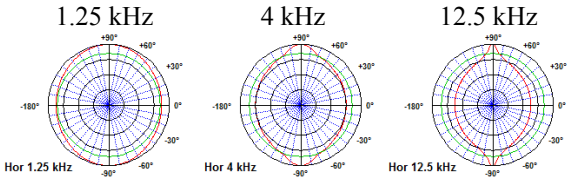

8.7. Legendre-shaded delay-curved CBT straight-line array:

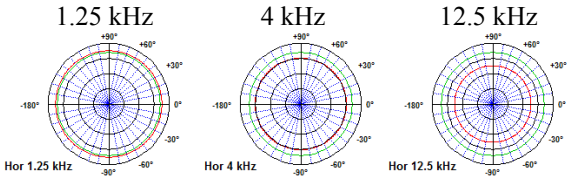

9. APPENDIX 4: TABLE: ARRAY PERFORMANCE RANKING

Array Type, Across: **Array Performance Parameter, Down:**	**(1)** **Un-shaded straight-line array**	**(2)** **Hann-shaded straight-line array**	**(3)** **Un-shaded "J"-line array**	**(4)** **Un-shaded spiral-line array**	**(5)** **Un-shaded circular-arc array**	**(6)** **Legendre-shaded CBT circular-arc array**	**(7)** **Legendre-shaded delay-curved CBT straight-line array**
Beamwidth uniformity:	2	2	1	9	8	10	10
Directivity uniformity:	1	1	4	7	5	10	10
Vertical sound-field uniformity:	1	4	2	2	4	10	10
Polar side lobe suppression:	1	9	6	7	7	10	10
Uniformity of polar response:	1	2	5	6	6	10	10
Smoothness and flatness of off-axis frequency response:	1	2	1	3	8	10	9
Sound pressure rolloff versus distance:	2	1	3	5	8	10	9
Near-far polar pattern uniformity:	1	2	4	7	8	10	9
TOTALS: (Scale 8 to 80)	**10**	**23**	**26**	**46**	**54**	**80**	**77**

The table yields the following ranking for the seven arrays:

1. CBT circular-arc array: 80,
2. CBT delay-curved straight-line array: 77,
3. Un-shaded circular-arc array: 54,
4. Spiral-line array: 46,
5. "J"-line array: 26,
6. Straight-line array (Hann shaded): 23, and
7. Straight-line array (not shaded): 10